NUREG/CR-1685, Vol. 2
HEDL-TME 80-72
RT

DYNAMIC ANALYSIS TO ESTABLISH NORMAL SHOCK AND VIBRATION OF RADIOACTIVE MATERIAL SHIPPING PACKAGES

QUARTERLY PROGRESS REPORT
APRIL 1, 1980 - JUNE 30, 1980

Hanford Engineering Development Laboratory

Operated by Westinghouse Hanford Company
P.O. Box 1970 Richland, WA 99352
A Subsidiary of Westinghouse Electric Corporation

S.R. Fields

Manuscript Completed: September 1980
Date Published: April 1981

Prepared for Division of Safeguards,
Fuel Cycle, and Environmental Research
Office of Nuclear Regulatory Research
U.S. Nuclear Regulatory Commission
Washington, DC 20555
NRC Fin No. B2263

NUREG/CR-1685, Vol. 2
HEDL-TME 80-72
RT

DYNAMIC ANALYSIS TO ESTABLISH NORMAL SHOCK AND VIBRATION OF RADIOACTIVE MATERIAL SHIPPING PACKAGES

Quarterly Progress Report
April 1, 1980 - June 30, 1980

S. R. Fields

ABSTRACT

An equation of motion was derived for an equivalent single-degree-of-freedom representation of the relative rotational motion between a radioactive material shipping package (cask) and its rail car (support). This equation of motion, along with those derived earlier for the relative horizontal and vertical motion, was used to construct CARRS (Cask-Rail Car Response Spectra Generator), a model to generate frequency response spectra using calculated results obtained from the CARDS (Cask Rail Car Dynamic Simulator) model. Frequency response spectra are presented for various exploratory cases. Further evaluation of the performance of CARDS was made, after insertion of the latest parameter data, by comparing calculated results with response variables measured during Test 3 of the series of tests conducted at the Savannah River Laboratories.

CONTENTS

	Page
Abstract	iii
Figures	vii
Tables	x
SUMMARY OF PROGRESS	1
INTRODUCTION	4
PROGRESS TO DATE	5
1. DEVELOP DYNAMIC MODEL	5
2. DATA COLLECTION AND REDUCTION	15
3. VALIDATE MODEL	15
4. COLLECT PARAMETER DATA	19
5. PARAMETRIC AND SENSITIVITY ANALYSIS	19
6. INTERIM REPORT	19
REFERENCES	21
APPENDIX A	A-1
Nomenclature of Terms	

FIGURES

Figure		Page
1	Spring-Mass Model of Cask-Rail Car System	22
2	Horizontal Acceleration of the Support for an Equivalent Single-Degree-of-Freedom System (Preliminary Cases 2, 3 and 4)	23
3	Vertical Acceleration of the Support for an Equivalent Single-Degree-of-Freedom System (Preliminary Cases 2, 3 and 4)	24
4	Rotational Acceleration of the Support for an Equivalent Single-Degree-of-Freedom System (Preliminary Cases 2, 3 and 4)	25
5	Response Spectrum: Maximum Absolute Relative Horizontal Acceleration vs Frequency (Preliminary Cases 1 through 5)	26
6	Response Spectrum: Maximum Absolute Relative Vertical Acceleration vs Frequency (Preliminary Cases 1 through 5)	27
7	Response Spectrum: Maximum Absolute Relative Rotational Acceleration vs Frequency (Preliminary Cases 1 through 5)	28
8	Coupler Force vs Time During Impact of Cask-Rail Car with Four Hopper Cars Loaded with Ballast (Test 3 - Instrument 3) (Case 1: Measured Coupler Force)	29
9	Horizontal Force of Interaction Between Cask and Rail Car vs Time During Impact with Four Hopper Cars Loaded with Ballast (Test 3 - Instrument 27) (Case 1: Measured Coupler Force)	30
10	Horizontal Acceleration of the Cask-Rail Car During Impact with Four Hopper Cars Loaded with Ballast (Test 3 - Instrument 12: Filtered at 100 Hz) (Case 1: Measured Coupler Force)	31
11	Horizontal Acceleration of the Cask During Impact with Four Hopper Cars Loaded with Ballast (Test 3 - Instrument 8: Filtered at 100 Hz) (Case 1: Measured Coupler Force)	32

FIGURES (Cont'd)

Figure		Page
12	Vertical Acceleration of the Cask at the Far End During Impact with Four Hopper Cars Loaded with Ballast (Test 3 - Instrument 11: Filtered at 50 Hz) (Case 1: Measured Coupler Force)	33
13	Vertical Acceleration of the Cask at the Struck End During Impact with Four Hopper Cars Loaded with Ballast (Test 3 - Instrument 9: Filtered at 50 Hz) (Case 1: Measured Coupler Force)	34
14	Vertical Displacements of the Cask During Impact with Four Hopper Cars Loaded with Ballast (Test 3) (Case 1: Measured Coupler Force)	35
15	Vertical Tiedown Forces During Impact with Four Hopper Cars Loaded with Ballast (Test 3) (Case 1: Measured Coupler Force)	36
16	Coupler Force vs Time During Impact of Cask-Rail Car with Four Hopper Cars Loaded with Ballast (Test 3 - Instrument 3) (Case 2: Calculated Coupler Force)	37
17	Horizontal Force of Interaction Between Cask and Rail Car vs Time During Impact with Four Hopper Cars Loaded with Ballast (Test 3 - Instrument 27) (Case 2: Calculated Coupler Force)	38
18	Horizontal Acceleration of the Cask-Rail Car During Impact with Four Hopper Cars Loaded with Ballast (Test 3 - Instrument 12: Filtered at 100 Hz) (Case 2: Calculated Coupler Force)	39
19	Horizontal Acceleration of the Cask During Impact with Four Hopper Cars Loaded with Ballast (Test 3 - Instrument 8: Filtered at 100 Hz) (Case 2: Calculated Coupler Force)	40
20	Vertical Acceleration of the Cask at the Far End During Impact with Four Hopper Cars Loaded with Ballast (Test 3 - Instrument 11: Filtered at 50 Hz) (Case 2: Calculated Coupler Force)	41
21	Vertical Acceleration of the Cask at the Struck End During Impact with Four Hopper Cars Loaded with Ballast (Test 3 - Instrument 9: Filtered at 50 Hz) (Case 2: Calculated Coupler Force)	42

FIGURES (Cont'd)

Figure		Page
22	Vertical Displacements of the Cask During Impact with Four Hopper Cars Loaded with Ballast (Test 3) (Case 2: Calculated Coupler Force)	43
23	Vertical Tiedown Forces During Impact with Four Hopper Cars Loaded with Ballast (Test 3) (Case 2: Calculated Coupler Force)	44

TABLES

Table		Page
1	Definitions of Cases Used for Generation of Preliminary Response Spectra	11
2	Theil's Inequality Coefficients for Response Variables Determined Using Calculated and Measured Coupler Force	18

DYNAMIC ANALYSIS TO ESTABLISH NORMAL SHOCK AND VIBRATION OF RADIOACTIVE MATERIAL SHIPPING PACKAGES

Quarterly Progress Report
April 1, 1980 - June 30, 1980

SUMMARY OF PROGRESS

1. DEVELOP DYNAMIC MODEL

Coupled equations of motion for the cask in the cask-rail car system in the CARDS (Cask Rail Car Dynamic Simulator) model were transformed into equations of motion for equivalent independent single-degree-of-freedom systems, one equation for each of the three directions of motion (i.e., horizontal, vertical and rotational). These equations of motion were used to construct CARRS (Cask Rail Car Response Spectra Generator), a model to generate frequency response spectra using calculated results obtained from CARDS.

Frequency response spectra were generated for various preliminary or exploratory cases defined by conditions and parameter values used in the CARDS and CARRS models. The response variables plotted as functions of frequency are the horizontal, vertical and rotational accelerations of a radioactive material shipping package (cask) relative to the corresponding accelerations of its support (rail car).

One of the conditions imposed on the system when the response spectra were generated was placement of the cask centerline 4 feet forward of the rail car centerline. This was compared to the case where the cask was centered fore and aft. It was found that the location of the cask on the rail car had little effect on the maximum absolute relative horizontal acceleration over the range of frequencies considered, but it had a great effect on the maximum absolute relative vertical acceleration. The relative vertical accelerations compared were those of the center-of-gravity (cg) of the cask relative to the cg of the rail car. However, there are higher relative vertical accelerations at other locations on the cask. Results from the CARDS model show that, for the centered cask case, the absolute relative vertical accelerations at the tiedown attachment points are almost 5 times greater than the corresponding accelerations at the cg.

Another of the conditions imposed on the system during generation of the response spectra was slack or "looseness" in the vertical component of the rear tiedowns. Results show that this slack had little effect on the maximum absolute relative horizontal acceleration, but that it produced significantly higher values of the maximum absolute relative vertical and rotational accelerations.

The effect of frictional damping opposing the horizontal motion of the cask relative to the rail car was also evaluated. This was done by comparing the results of the damped case with the results of an undamped case. The results show that frictional damping decreases the maximum absolute relative horizontal acceleration, but has little effect on the maximum absolute relative vertical and rotational accelerations.

The response spectra generated are presented as maximum absolute relative accelerations vs frequency in Figures 5, 6 and 7.

Support accelerations, i.e., the forcing functions on the right hand sides of the equivalent independent single-degree-of-freedom equations of motion, are presented as functions of time in Figures 2, 3 and 4.

3. VALIDATE MODEL

Parameter data supplied by ENSCO, Incorporated under Task 4 (COLLECT PARAMETER DATA) of this study were inserted in the CARDS model to establish a base case for model validation and for planned parametric and sensitivity analyses. Simulation runs were then made to obtain new calculated results to be compared with the experimental results obtained from Tests 3 and 4 of the series conducted at the Savannah River Laboratories (SRL) in July and August of 1978.

An evaluation of the performance of the CARDS model was made by comparing calculated results with six response variables measured during Test 3 of the SRL series. Comparisons were made for two cases, one using measured coupler force as the excitation force, and one using the coupler force calculated by CARDS. Acceptable quantitative agreement, in terms of Theil's inequality coefficients, was obtained for all the response variables, except for the vertical accelerations of the cask at the struck and far ends. However, good visual agreement was obtained for these accelerations when their time traces were compared. If it were not for time shifts of about 0.02 to 0.025 second, the calculated and experimental time traces would be brought into better alignment which would, in turn, produce more acceptable quantitative agreement.

Good agreement between the calculated and experimental results was obtained only after allowance was made for slack in the vertical tiedown structure at the far end. This slack, or looseness, in the tiedowns is clearly evident in high speed films of the tests. The films show rain water being ejected from the collar at the far end of the cask at impact. Also, it was recalled that a rubber shim had been installed between the collar and the cask. When this gap and rubber shim combination was considered as part of the tiedown structure, and an appropriate non-linear stiffness coefficient devised, good agreement between the calculated and experimental results was obtained. Confirmation of the existence of this slack in the tiedown structure was obtained by comparing the calculated vertical displacement of the cask at the far end with the corresponding displacement obtained by double integration of the measured vertical acceleration of the cask.

INTRODUCTION

The objective of this study is to determine the extent to which the shocks and vibrations experienced by radioactive material shipping packages during normal transport conditions are influenced by or are sensitive to various structural parameters of the transport system (i.e., package, package supports, and vehicle). The purpose of this effort is to identify those parameters which significantly affect the normal shock and vibration environments so as to provide the basis for determining the forces transmitted to radioactive material packages. Determination of these forces will provide the input data necessary for a broad range of package-tiedown structural assessments.

Progress on this study from April 1, 1980 to June 30, 1980 will now be discussed.

PROGRESS TO DATE

This study is divided into six tasks as discussed in previous progress reports. Progress on each of these tasks will now be discussed.

1. DEVELOP DYNAMIC MODEL

Equations of motion were derived for equivalent single degree-of-freedom (1-DOF) representations of the relative horizontal, vertical and rotational motion between a radioactive material shipping package and its rail car (support). These equations of motion (EOMs) were used to construct CARRS (Cask Rail Car Response Spectra Generator), a model to generate frequency response spectra using calculated results obtained from the CARDS (Cask Rail Car Dynamic Simulator) model. The cask-rail car system simulated by CARDS is shown in Figure 1.

Response spectra for the cask-rail car system are obtained by converting the coupled EOMs for the cask in the CARDS model into EOMs for equivalent independent 1-DOF systems. The procedure for making this conversion is patterned after that of Harris and Crede.[1] Equivalent independent 1-DOF equations describing the relative horizontal and vertical motion between the cask and rail car, derived using this procedure, are presented in Reference 2. These equations are

$$
\begin{aligned}
\ddot{Y}_d + \omega_Y^2 Y_d + \frac{(C_{S2} + C_{S3})}{M_P}\dot{Y}_d = \ddot{Y}_{RC} &+ \frac{(k_{S3}\ell_{CF} - k_{S2}\ell_{CR})}{M_P}\theta_{RC} \\
&+ \frac{(k_{S2} - k_{S3})}{M_P}\ell_{PR}\theta_P \\
&+ \frac{(C_{S3}\ell_{CF} - C_{S2}\ell_{CR})}{M_P}\dot{\theta}_{RC} \\
&+ \frac{(C_{S2} - C_{S3})}{M_P}\ell_{PR}\dot{\theta}_P \qquad (1)
\end{aligned}
$$

for the relative vertical motion, and

$$\ddot{X}_d + \omega_X^2 X_d + \frac{(C_{S1} + C_{S4})\dot{X}_d}{M_p} + \frac{\mu_{PR}(W_{P1} + W_{P4})\mathrm{sgn}(\dot{X}_d)}{M_p}$$

$$= \ddot{X}_{RC} - \omega_X^2 (Z_{RC}\theta_{RC} + Z_P\theta_P) - \frac{(C_{S1} + C_{S4})(Z_{RC}\dot{\theta}_{RC} + Z_P\dot{\theta}_P)}{M_p} \qquad (2)$$

for the relative horizontal motion. A nomenclature of terms used in this report is presented in the Appendix.

An equivalent independent 1-DOF equation describing the relative rotational motion between the cask and rail car will now be derived using the same procedure used in Reference (2) to get Equations (1) and (2). In the CARDS model, the equation of motion for rotational motion of the cask is expressed as

$$I_P\ddot{\theta}_P = Z_P(DUS1 + DUS4 - DWS1 - DWS4) - \ell_{PR}(DUS2-DWS2) + \ell_{PF}(DUS3 - DWS3) \qquad (3)$$

where

$$DUS1 = -k_{S1}[(X_{RC} + Z_{RC}\theta_{RC}) - (X_P - Z_P\theta_P)] \qquad (4)$$

$$DUS2 = -k_{S2}[(Y_{RC} + \ell_{CR}\theta_{RC}) - (Y_P + \ell_{PR}\theta_P)] \qquad (5)$$

$$DUS3 = -k_{S3}[(Y_{RC} - \ell_{CF}\theta_{RC}) - (Y_P - \ell_{PF}\theta_P)] \qquad (6)$$

$$DUS4 = -k_{S4}[(X_{RC} + Z_{RC}\theta_{RC}) - (X_P - Z_P\theta_P)] \qquad (7)$$

$$DWS1 = C_{S1}[(\dot{X}_{RC} + Z_{RC}\dot{\theta}_{RC}) - (\dot{X}_P - Z_P\dot{\theta}_P)] \tag{8}$$

$$DWS2 = C_{S2}[(\dot{Y}_{RC} + \ell_{CR}\dot{\theta}_{RC}) - (\dot{Y}_P + \ell_{PR}\dot{\theta}_P)] \tag{9}$$

$$DWS3 = C_{S3}[(\dot{Y}_{RC} - \ell_{CF}\dot{\theta}_{RC}) - (\dot{Y}_P - \ell_{PF}\dot{\theta}_P)] \tag{10}$$

Combining Equations (3) through (10) gives

$$\begin{aligned} I_P\ddot{\theta}_P = & -Z_P(k_{S1} + k_{S4})[(X_{RC} + Z_{RC}\theta_{RC}) - (\ddot{X}_P - Z_P\theta_P)] \\ & + k_{S2}\ell_{PR}[(Y_{RC} + \ell_{CR}\theta_{RC}) - (Y_P + \ell_{PR}\theta_P)] \\ & - k_{S3}\ell_{PF}[(Y_{RC} - \ell_{CF}\theta_{RC}) - (Y_P - \ell_{PF}\theta_P)] \\ & - Z_P(C_{S1} + C_{S4})[(\dot{X}_{RC} + Z_{RC}\dot{\theta}_{RC}) - (\dot{X}_P - Z_P\dot{\theta}_P)] \\ & + C_{S2}\ell_{PR}[(\dot{Y}_{RC} + \ell_{CR}\dot{\theta}_{RC}) - (\dot{Y}_P + \ell_{PR}\dot{\theta}_P)] \\ & - C_{S3}\ell_{PF}[(\dot{Y}_{RC} - \ell_{CF}\dot{\theta}_{RC}) - (\dot{Y}_P - \ell_{PF}\dot{\theta}_P)] \end{aligned} \tag{11}$$

Let the relative horizontal displacement be defined as

$$\theta_d = \theta_{RC} - \theta_P \tag{12}$$

The relative rotational velocity and acceleration are then

$$\dot{\theta}_d = \dot{\theta}_{RC} - \dot{\theta}_P \tag{13}$$

and

$$\ddot{\theta}_d = \ddot{\theta}_{RC} - \ddot{\theta}_P \tag{14}$$

Combining Equations (11) through (14) gives, after much algebra, the following EOM in terms of the relative displacment θ_d

$$\ddot{\theta}_d + \omega_\Theta^2\theta_d + \xi_\theta\dot{\theta}_d = \ddot{\theta}_{RC} + \omega_\theta^2\theta_{RC} + \xi_\theta\dot{\theta}_{RC} - \psi_\theta \tag{15}$$

The frequency, ω_θ, is defined by

$$\omega_\theta^2 = \frac{Z_P^2\,(k_{S1} + k_{S4}) + k_{S2}\ell_{PR}^2 + k_{S3}\ell_{PF}^2}{I_P} \tag{16}$$

The term ξ_θ is a damping coefficient defined as

$$\xi_\theta = \frac{Z_P^2\,(C_{S1} + C_{S4}) + C_{S2}\ell_{PR}^2 + C_{S3}\ell_{PF}^2}{I_P} \tag{17}$$

The remaining term, ψ_θ, is a coupling term. It is expressed in terms of the coordinates X_{RC}, Y_{RC}, and θ_{RC} describing the motion of the rail car, and the two remaining coordinates X_P and Y_P describing the horizontal and vertical motion of the cask. This coupling term is defined as

$$\begin{aligned}
\psi_\theta = \Big\{ & - Z_P(k_{S1} + k_{S4})[(X_{RC} + Z_{RC}\theta_{RC}) - X_P] \\
& + k_{S2}\ell_{PR}[(Y_{RC} + \ell_{RC}\theta_{RC}) - Y_P] \\
& - k_{S3}\ell_{PF}[(Y_{RC} - \ell_{CF}\theta_{RC}) - Y_P] \\
& - Z_P(C_{S1} + C_{S4})[(\dot{X}_{RC} + Z_{RC}\dot{\theta}_{RC}) - \dot{X}_P] \\
& + C_{S2}\ell_{PR}[(\dot{Y}_{RC} + \ell_{CR}\dot{\theta}_{RC}) - \dot{Y}_P] \\
& - C_{S3}\ell_{PF}[(\dot{Y}_{RC} - \ell_{CF}\dot{\theta}_{RC}) - \dot{Y}_P]\Big\} / I_P
\end{aligned} \tag{18}$$

Equations (1), (2) and (15) are independent 1-DOF EOMs with forcing functions defined by the right hand sides (RHSs) of the respective equations. If it is assumed that the RHS of each 1-DOF EOM represents the time-varying acceleration of a platform supporting a 1-DOF device defined by the left hand side (LHS) of the respective EOM, then the response of the device to various platform or support motions may be studied. If the RHSs of Equations (1), (2) and (15) are defined as

$$\ddot{Y}_S = \ddot{Y}_{RC} + \frac{(k_{S3}\ell_{CF} - k_{S2}\ell_{CR})\theta_{RC}}{M_P} + \frac{(k_{S2} - k_{S3})\ell_{PR}\theta_P}{M_P}$$

$$+ \frac{(C_{S3}\ell_{CF} - C_{S2}\ell_{CR})\dot{\theta}_{RC}}{M_P} + \frac{(C_{S2} - C_{S3})\ell_{PR}\dot{\theta}_P}{M_P} \qquad (19)$$

$$\ddot{X}_S = \ddot{X}_{RC} - \omega_X^2 (Z_{RC}\theta_{RC} + Z_P\theta_P) - \frac{(C_{S1} + C_{S4})(Z_{RC}\dot{\theta}_{RC} + Z_P\dot{\theta}_P)}{M_P} \qquad (20)$$

and

$$\ddot{\theta}_S = \ddot{\theta}_{RC} + \omega_\theta^2\theta_{RC} + \xi_\theta\dot{\theta}_{RC} - \psi_\theta \qquad (21)$$

respectively, then the 1-DOF EOMs may be expressed as

$$\ddot{Y}_d + \omega_Y^2 Y_d + \frac{(C_{S2} + C_{S3})\dot{Y}_d}{M_P} = \ddot{Y}_S \qquad (22)$$

$$\ddot{X}_d + \omega_X^2 X_d + \frac{(C_{S1} + C_{S4})\dot{X}_d}{M_P} + \frac{\mu_{PR}}{M_P}(W_{P1} + W_{P4})\,\mathrm{sgn}\,(\dot{X}_d) = \ddot{X}_S \qquad (23)$$

and

$$\ddot{\theta}_d + \omega_\theta^2\theta_d + \xi_\theta\dot{\theta}_d = \ddot{\theta}_S \qquad (24)$$

where

$\ddot{Y}_S$ = the vertical acceleration of the support, L/θ^2
$\ddot{X}_S$ = the horizontal acceleration of the support, L/θ^2
$\ddot{\theta}_S$ = the rotational acceleration of the support, $1/\theta^2$

Assuming that the motion of a support is not influenced by the device attached to it, the response spectra of the device may be determined by varying the frequencies on the LHSs of Equations (22), (23) and (24).

Equations (22), (23) and (24) were used to construct the response spectra generator model CARRS. The support accelerations, defined by Equations (19), (20) and (21), are determined as functions of time by the CARDS model during a simulation, and written on a file to be read later by the CARRS model to generate the response spectra.

Response spectra are generated by the CARRS model in the following manner. Time-varying support accelerations (the RHSs of the 1-DOF EOMs in CARRS) are read from the file created by CARDS until arrays are filled. These arrays are then accessed at each time interval as the transient progresses. A common frequency is then set for the LHSs of the 1-DOF EOMs. The support accelerations are then traversed over the complete transient and the relative horizontal, vertical and rotational accelerations computed. The frequency on the LHSs of the 1-DOF EOMs is then set at a different value, the integrators are re-initialized, and the transient traversed again to obtain new values of the relative accelerations. This procedure was repeated for frequencies of 2, 5 and 10 through 260 Hz, in 10 Hz increments. The entire frequency range was covered, for a particular set of support accelerations, by successive CARRS runs chained together as one run. A set of maximum or peak relative accelerations for each frequency was automatically determined by CARRS. Response spectra were then obtained by plotting the absolute values of these maximum accelerations against the frequency.

Response spectra were generated for various preliminary or exploratory cases based on certain conditions and parameter values used in the CARDS and CARRS models. These cases are defined in Table 1

TABLE 1

DEFINITIONS OF CASES USED FOR GENERATION OF PRELIMINARY RESPONSE SPECTRA

CONDITION *	CASE				
	1	2	3	4	5
1. Rear Tiedowns					
- Loose	X				
- Tight		X	X	X	X
2. Cask Position on Rail Car					
- Centered Fore & Aft					X
- Cask Centerline 4 ft Forward of Rail Car Centerline	X	X	X	X	
3. Coupler Force Used					
- Calculated by CARDS					
- Measured During SRL Tests	X	X	X	X	X
4. Damping in CARDS Model					
- Viscous + Friction**	X	X	X	X	X
- Viscous Only					
- No Damping					
5. Damping in CARRS Model					
- Viscous + Friction**	X	X			
- Viscous Only				X	
- No Damping			X		X

*Conditions not specified here are base case conditions in the CARDS model.
**Friction opposing horizontal motion of cask relative to the rail car.

The cases defined in Table 1 differ due to only three of the conditions listed. The only difference between Cases 1 and 2 is due to the condition of the rear tiedowns. Case 1 represents the condition of the rear tiedowns in Tests 3 and 4 of the coupling tests conducted at the Savannah River Laboratories (SRL) in July and August of 1978. In the previous progress report,[2] it was stated that ENSCO, Incorporated had completed a study to provide parameter data on the railway equipment used in the coupling tests conducted at SRL. These data were used to establish the base case for simulation of Tests 3 and 4 using the CARDS model. After experiencing difficulty in matching the vertical acceleration of the cask at the far end (as determined using the CARDS model) with that measured during the tests, high speed films of the tests were examined for some indication of the reason for the mismatch (see Section 3. VALIDATE MODEL). The films showed that water (rain water collected during a rain storm the previous night) was ejected from the collar around the cask at the far end. It was also recalled that a rubber bushing or liner had been installed between the cask and the collar. These conditions indicated a possible loose fit between the cask and the collar. Because this cask and collar combination is part of the tiedown system at the far end, it was concluded that the mismatch of results was due to looseness in the rear tiedowns. This was confirmed by integrating the cask acceleration recorded during the tests twice with respect to time to get cask displacement, and then comparing this displacement to the calculated displacement. It was found that the calculated displacement matched the "integrated-measured" displacement reasonably well only by assuming an initial "free" or loose rear tiedown, followed by contact with a rubber bushing, and finally followed by "solid" contact with rubber compressed against the collar. Case 2 represents a condition where neither slack nor a rubber bushing exists in the rear tiedowns, i.e., the rear tiedowns are as tight as the front tiedowns.

Case 2 is, in effect, the base case for Cases 1, 3, 4 and 5. Case 2 represents a set of conditions including:

(1) no looseness in the vertical component of the rear (or front) tiedowns,

(2) the cask centerline is positioned 4 feet forward of the rail car centerline,

(3) the time-varying coupler force is that measured during the SRL tests,

(4) damping in the equations of motion in the CARDS model includes both viscous (structural) damping and damping due to friction opposing the horizontal motion of the cask relative to the rail car, and

(5) damping in the 1-DOF EOMs in the CARRS model is the same as that of Item (4) above.

Case 3 differs from Case 2 due to a change in condition (5) above, i.e., there is no damping of any kind in the 1-DOF EOMs in CARRS. The only difference between Case 4 and Case 2 is also due to a change in condition (5), however, in Case 4, there is viscous (structural) damping only. Finally, Case 5 differs from Case 2 due to condition (2), i.e., the cask is centered fore and aft on the rail car rather than being shifted 4 feet forward of this position, as in the SRL tests.

The support accelerations [defined by Equations (19), (20), and (21)] calculated by CARDS are presented in Figures 2, 3 and 4. Figure 2 is a plot of the horizontal acceleration of the support for the equivalent 1-DOF system, as a function of time, for Cases 2, 3 and 4. Figures 3 and 4 are the corresponding plots for the vertical and rotational accelerations of the support, respectively. The support accelerations for Cases 1 and 5 are different than those shown in Figures 2, 3 and 4 because the differences in conditions (1) and (2) in Table 1 required separate CARDS simulations, which produced different results. The support accelerations of Figures 2, 3 and 4 are presented as typical examples of the RHS forcing functions used in the 1-DOF EOMs in CARRS.

The response spectra generated by the CARRS model, for the "preliminary" cases defined in Table 1, are presented in Figures 5, 6 and 7.

Figure 5 consists of plots of the maximum absolute relative (MAR) horizontal acceleration of the equivalent 1-DOF system as a function of frequency [see Equations (2)]. Figures 6 and 7 are the corresponding frequency plots of the maximum absolute relative vertical and rotational accelerations, respectively. In Figure 5, Cases 3 and 5 produce almost identical plots with the highest accelerations over the range of frequencies considered. These plots have a common maximum value of the maximum (maximax) absolute relative horizontal acceleration of about 8500 in/sec^2 at a frequency of 250 Hz. The significance of the identical plots produced by Cases 3 and 5 is that the only difference between these cases is the positioning of the cask on the rail car (see Table 1). Case 3 has the cask centerline positioned 4 feet forward of the rail car centerline, while Case 5 has the cask centered fore and aft. The conclusion may be drawn that this difference in the location of the cask on the rail car has little effect on the maximum absolute relative horizontal acceleration over the range of frequencies considered. However, the location of the cask on the rail car has a great effect on the maximum absolute relative vertical acceleration, as shown in Figure 6. A maximax absolute relative vertical acceleration of about 5300 in/sec^2, at a frequency of 50 Hz, is obtained for Case 3, while the maximum (not maximax) absolute relative vertical acceleration obtained for Case 5 is less than 100 in/sec^2 over the entire frequency range. It should be pointed out here that these accelerations are the relative vertical accelerations of the center-of-gravity (cg) of the cask relative to the cg of the rail car. There are higher relative vertical accelerations at other locations on the cask. Results from the CARDS model show that, for the centered cask case (Case 5), the absolute relative vertical accelerations of the cask at the tiedown attachment points are about 280 in/sec^2, while the corresponding absolute relative vertical acceleration at the cg is about 62 in/sec^2. The absolute relative vertical accelerations at the tiedown attachment points are almost 5 times greater than the corresponding accelerations at the cg.

The plots for Cases 1 and 2 in Figure 5 are close together which indicates that looseness in the vertical component of the rear tiedowns has little effect on the maximum absolute relative horizontal acceleration. In contrast, the plots for Cases 1 and 2 in Figure 6 are widely separated, indicating that this looseness in the rear tiedowns produces significantly higher values of the maximum absolute relative vertical acceleration at all frequencies. Vertical looseness in the rear tiedowns also produces substantially greater maximum absolute relative (MAR) rotational accelerations, as shown in Figure 7. Figure 7 shows widely separated plots for Cases 1 and 2, with Case 1 having the higher accelerations over the range of frequencies considered.

The effect of frictional damping opposing the horizontal motion of the cask relative to the rail car is illustrated by the plots for Cases 2 and 4 in Figures 5, 6 and 7. In Figure 5, separation of the plots for Cases 2 and 4 shows that frictional damping decreases the MAR horizontal acceleration over most of the frequency range. The lower plot in Figure 5 consists of the results for Case 2, the case where frictional damping is present along with viscous (structural) damping. The results of Case 4 are presented as the upper plot in Figure 5. This case has viscous damping, but no frictional damping. Frictional damping has little effect on the MAR vertical acceleration and on the MAR rotational acceleration, as indicated by the superposition of points on the plots for Cases 2 and 4 in Figures 6 and 7, respectively.

2. DATA COLLECTION AND REDUCTION

There has been no activity in this task during this reporting period.

3. VALIDATE MODEL

In a previous report,[3] it was shown that results obtained from a CARDS simulation of Test 3 of the SRL c ling tests were in good agreement with experimental results except for e vertical accelerations of the cask. In the following reporting period,[2] ENSCO, Incorporated completed a study to provide parameter data on the railway equipment used in the coupling tests at SRL. These data were inserted in the CARDS model to establish a base case for model validation and for planned parametric and sensitivity analyses. Additional simulation runs were made to obtain new calculated results to be compared with the experimental results.

At first, the new data resulted in less agreement between the calculated and experimental results than had been obtained previously. The calculated and experimental values of the vertical acceleration of the cask at the far end did not show acceptable agreement when compared both visually and quantitatively. After modifications were made to the model, based on a review of high speed films of the tests and of system structural features, a dramatic improvement in the agreement was realized (especially in the visual comparisons). The high speed films of Test 3 showed that water was ejected from the collar around the cask at the far end at impact (rain water had collected under the collar during a rain storm the night before the test). It was also recalled that a rubber gasket or shim was used under the collar. This suggested that the rubber, or a gap, or both, could cause both an increase in the magnitude and frequency of the acceleration readings at the far end, precisely the characteristics needed to achieve agreement. Double integration of the measured accelerations gave displacements which confirmed this conclusion. Therefore, a non-linear stiffness coefficient was devised for the rear tiedowns that was assumed to consist of a series combination of an initial gap between the cask and its collar, a rubber shim, and then the intended tiedown structure. A corresponding damping coefficient was also devised.

As in the preliminary assessment of Reference 3, the latest assessment of how well the CARDS model simulates the behavior of the cask-rail car system for the conditions of Test 3 of the SRL experiments was made by comparing, for two cases, both visually and quantitatively, the calculated and experimental values of coupler force, the longitudinal force of interaction between the cask and rail car, the horizonal acceleration of the rail car, the horizontal acceleration of the cask, the vertical acceleration of the cask at the far end, and the vertical acceleration of the cask at the struck end. Also, in this latest assessment, the calculated vertical displacements of the cask were compared to those obtained by double integration of the measured vertical accelerations of the cask. In both cases, the coupler force was the force of excitation causing the system to vibrate. In the first case (Case 1), the experimentally measured coupler force was used. In the second case (Case 2), the coupler force used was that calculated by the CARDS model. Visual comparisons are presented in Figures 8 through 14 for Case 1, and in Figures 16 through 22 for Case 2. To supplement these comparisons, calculated vertical tiedown forces are presented in Figure 15 for Case 1, and in Figure 23 for Case 2. Quantitative comparisons of each pair of individual response variables were made using Theil's two-variable inequality coefficients. A simultaneous quantitative comparison of all the response variables was made using Theil's multiple inequality coefficient. The quantitative comparisons are summarized in Table 2. Theil's two-variable inequality coefficients are discussed in Reference 3 and 4, and Theil's multiple inequality coefficient is discussed in References 3 and 5.

The Theil's inequality coefficients in Table 2 show that good agreement between calculated and experimental results was obtained for all but the vertical accelerations. The vertical accelerations of the cask produced two-variable inequality coefficients above 0.5 (Theil's inequality coefficients are zero at perfect agreement and 1 at the poorest agreement). However, Figures 12, 13, 20 and 21 show that good visual agreement exists between the vertical accelerations. Both the magnitude and frequency of these plots are in good agreement. It appears, however, that better quantitative agreement could be obtained if the calculated vertical acceleration at the far end (Figures 12 and 20) could be made to shift approximately 0.025 second forward on the time scale, and if the calculated vertical acceleration at the struck end (Figures 13 and 21) could be shifted about 0.02 second backward on the time scale. Theil's multiple inequality coefficient for Case 1 is 0.059, and that for Case 2 is 0.214.

TABLE 2

THEIL'S INEQUALITY COEFFICIENTS FOR RESPONSE VARIABLES DETERMINED USING CALCULATED AND MEASURED COUPLER FORCE

Response Variable	Case 1	Case 2
	Measured Coupler Force	Calculated Coupler Force
	Theil's Two-Variable Inequality Coefficients*	Theil's Two-Variable Inequality Coefficients*
Coupler Force	0.	0.223
Longitudinal Force of Interaction Between Cask and Railcar	0.158	0.194
Horizontal Acceleration of Cask	0.205	0.252
Horizontal Acceleration of Railcar	0.211	0.445
Vertical Acceleration of Cask at Far End	0.600	0.776
Vertical Acceleration of Cask at Struck End	0.656	0.470
Theil's Multiple Inequality Coefficient	0.059	0.214

*A value of 0 indicates the best agreement and a value of 1 indicates the poorest agreement.

The plots of calculated vertical acceleration of the cask at the far end in Figures 12 and 20 are shaped by the non-linear stiffness coefficient devised for the rear tiedowns. Initially, the cask accelerates freely upward due to the loose fit of the collar, but then it soon encounters the rubber-cushioned collar and decelerates rapidly. The stiffness coefficient of the rubber shim varies with relative displacement, therefore, the frequency varies. The structural damping of the collar varies in a manner similar to that of the stiffness coefficient.

The vertical displacements of the cask are presented in Figures 14 and 22. These figures compare the calculated vertical displacements with those obtained by double integration of the measured vertical accelerations of the cask. Figure 14 presents the comparisons of Case 1 results, and Figure 22 the comparisons of Case 2 results. Both of these figures show good agreement up to about 0.1 second, and then the calculated and "experimental" displacement curves show substantial separation. The reason for this separation will be sought in subsequent simulations.

4. COLLECT PARAMETER DATA

There has been no activity in this task during this reporting period.

5. PARAMETRIC AND SENSITIVITY ANALYSIS

A limited parametric analysis, using the CARDS and CARRS models, was conducted to generate frequency response spectra for various preliminary or exploratory cases (see Section 1. DEVELOP DYNAMIC MODEL).

6. INTERIM REPORT

There has been no activity in this task during this reporting period.

REFERENCES

1. C. M. Harris and C. Crede, Shock and Vibration Handbook, Vol. 2 (page 31-2) and Vol. 3 (page 50-10), McGraw-Hill, 1961.

2. S. R. Fields, Dynamic Analysis to Establish Normal Shock and Vibration of Radioactive Material Shipping Packages, NUREG/CR-1685, Vol. 1, (HEDL-TME 80-51), Quarterly Progress Report (January 1, 1980 - March 31, 1980), January 1981.*

3. S. R. Fields and S. J. Mech, Dynamic Analysis to Establish Normal Shock and Vibration of Radioactive Material Shipping Packages, NUREG/CR-1484, (HEDL-TME 80-24), Quarterly Progress Report (October 1, 1979 - December 31, 1979), March 1980.*

4. S. R. Fields and S. J. Mech, Dynamic Analysis to Establish Normal Shock and Vibration of Radioactive Material Shipping Packages, NUREG/CR-0880, (HEDL-TME 79-29), Quarterly Progress Report (January 1, 1979 - March 31, 1979), September 1979.*

5. S. R. Fields and S. J. Mech, Dynamic Analysis to Establish Normal Shock and Vibration of Radioactive Material Shipping Packages, NUREG/CR-1066, (HEDL-TME 79-43), Quarterly Report (April 1, 1979 - June 30, 1979), October 1979.*

*Available for purchase from the NRC/GPO Sales Program, U.S. Nuclear Regulatory Commission, Washington, DC 20555, and/or the National Technical Information Service, Springfield, VA 22161.

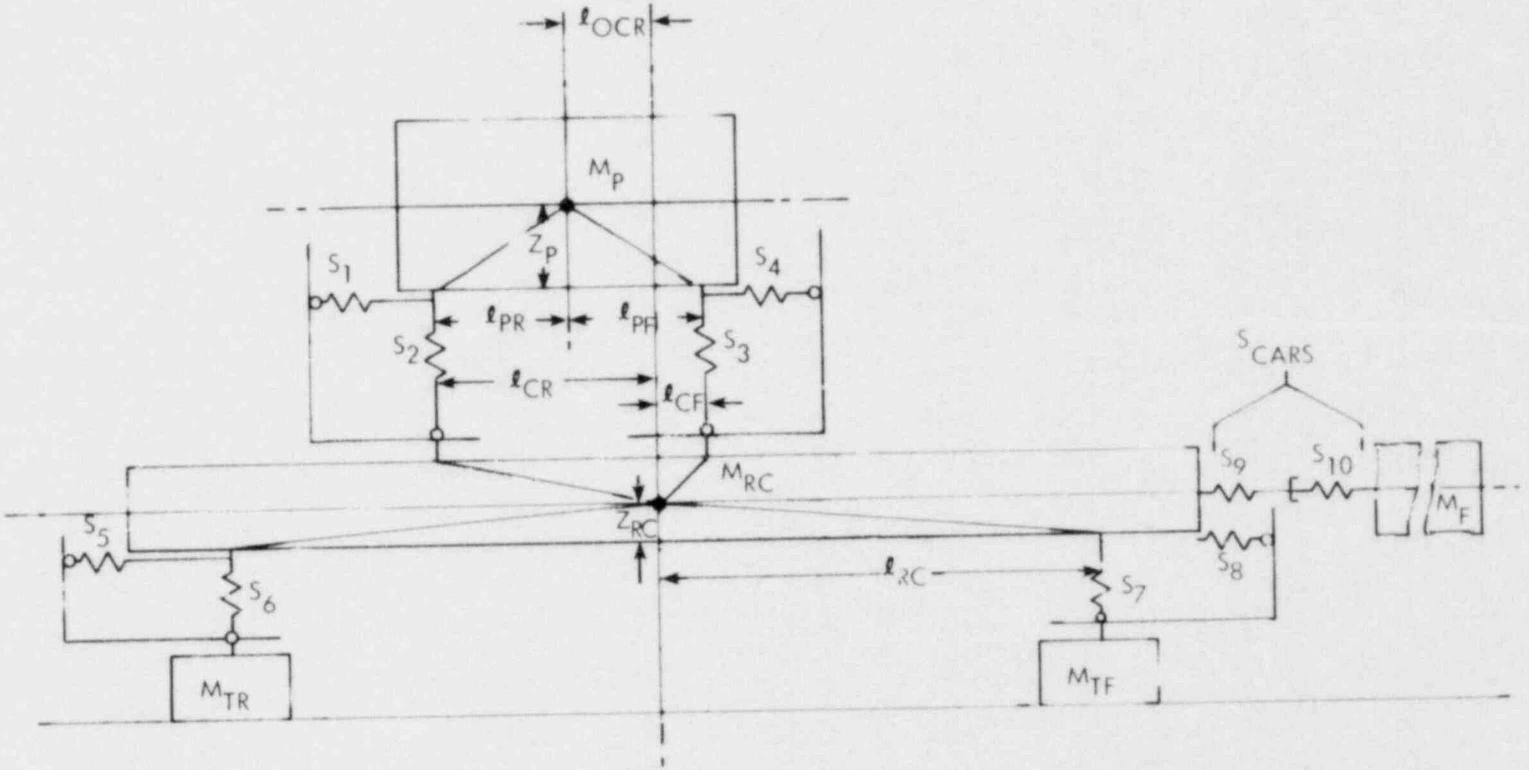

HEDL 7803-106.4

FIGURE 1. Spring-Mass Model of Cask-Rail Car System.

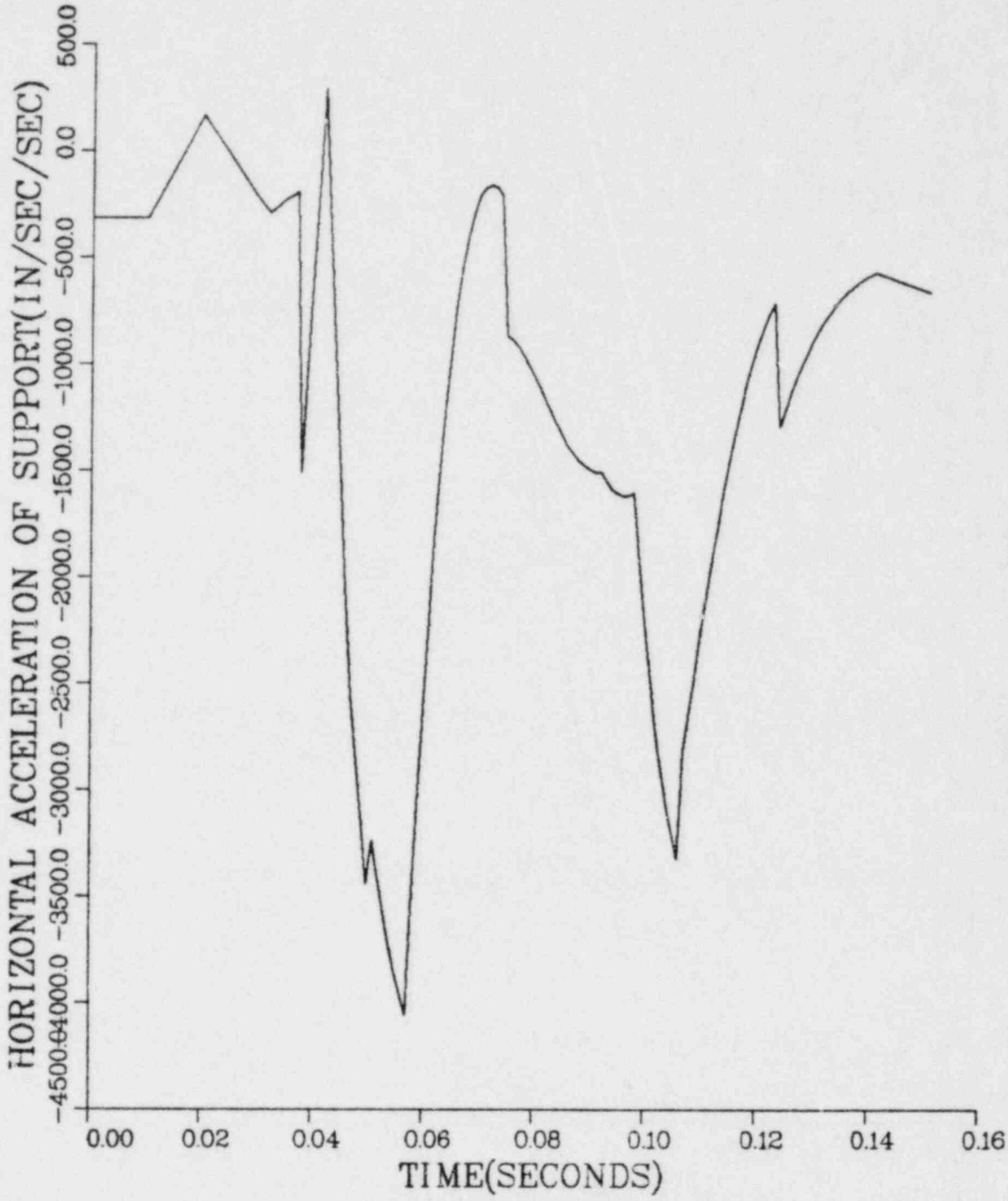

FIGURE 2. Horizontal Acceleration of the Support for an Equivalent Single-Degree-of-Freedom System (Preliminary Cases 2, 3 and 4).

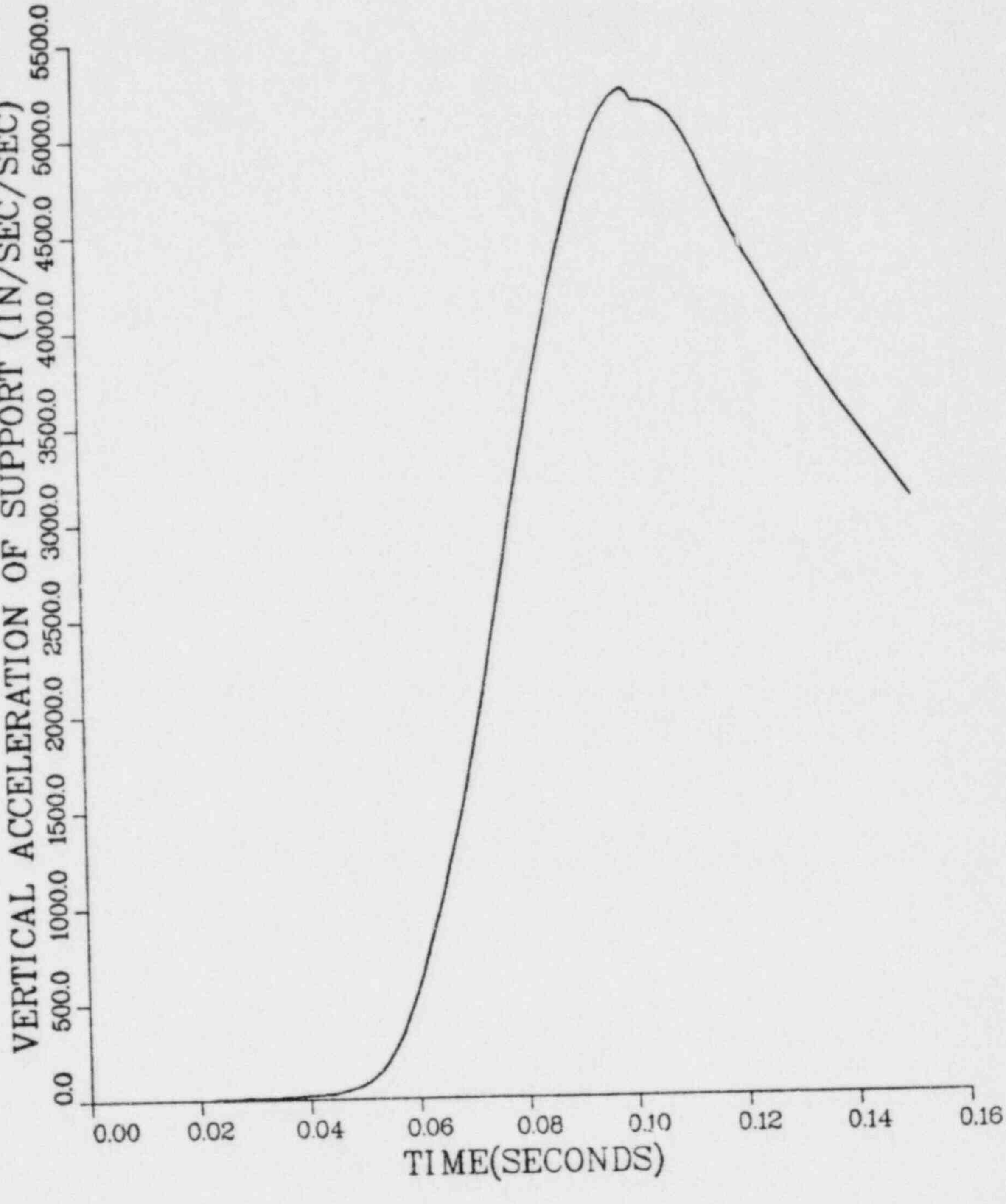

FIGURE 3. Vertical Acceleration of the Support for an Equivalent Single-Degree-of-Freedom System (Preliminary Cases 2, 3 and 4).

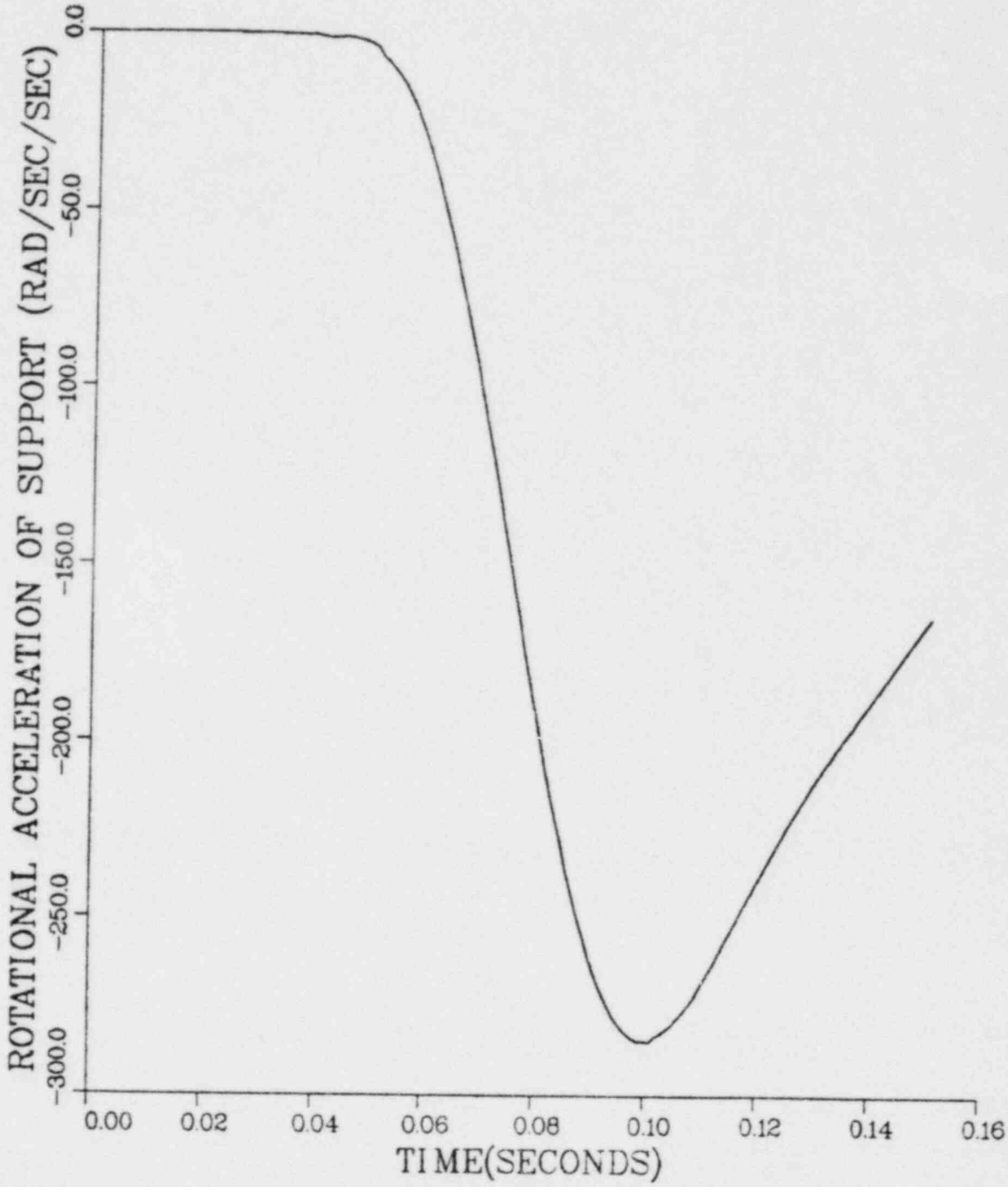

FIGURE 4. Rotational Acceleration of the Support for an Equivalent Single-Degree-of-Freedom System (Preliminary Cases 2, 3 and 4).

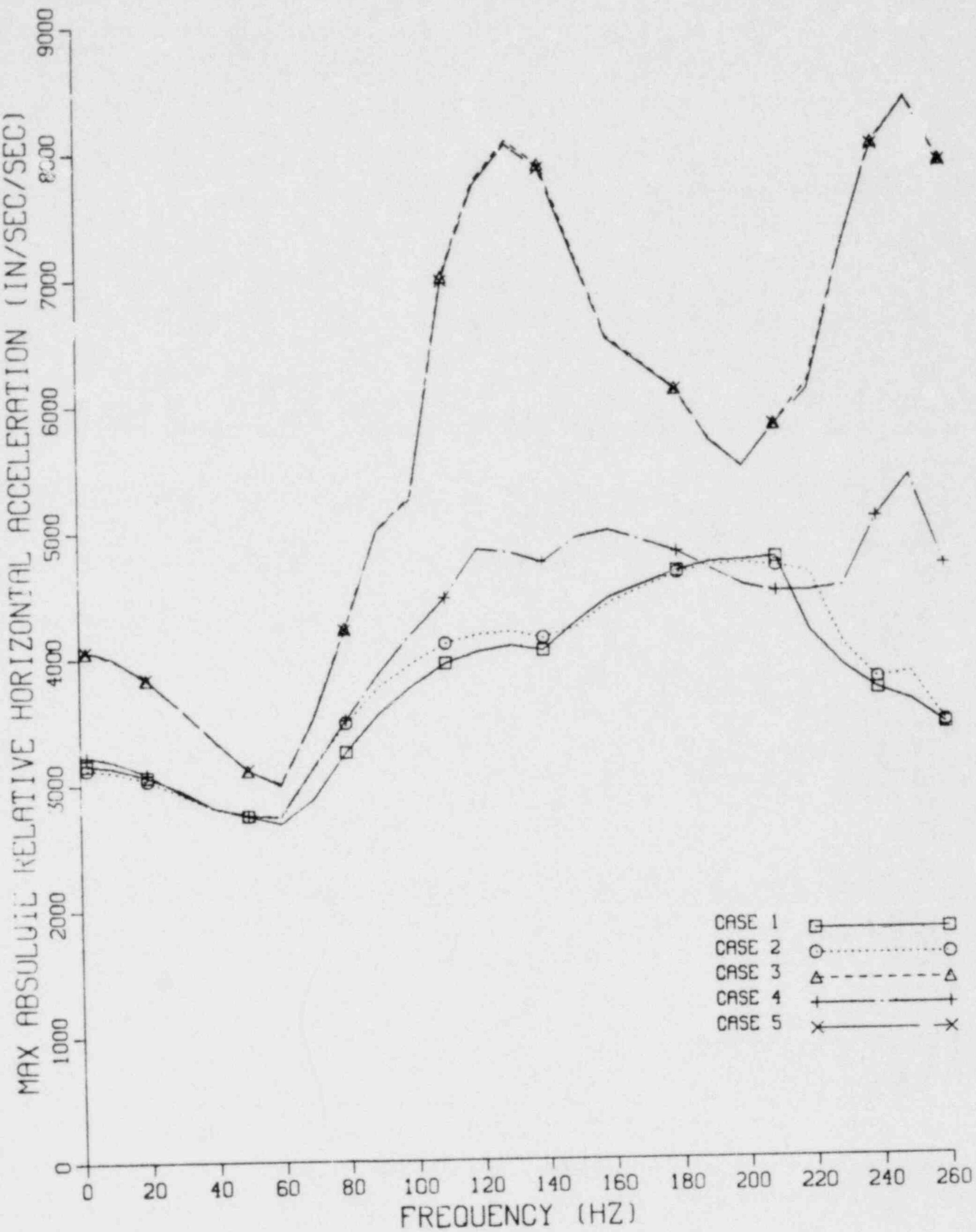

FIGURE 5. Response Spectrum: Maximum Absolute Relative Horizontal Acceleration vs Frequency (Preliminary Cases 1 through 5).

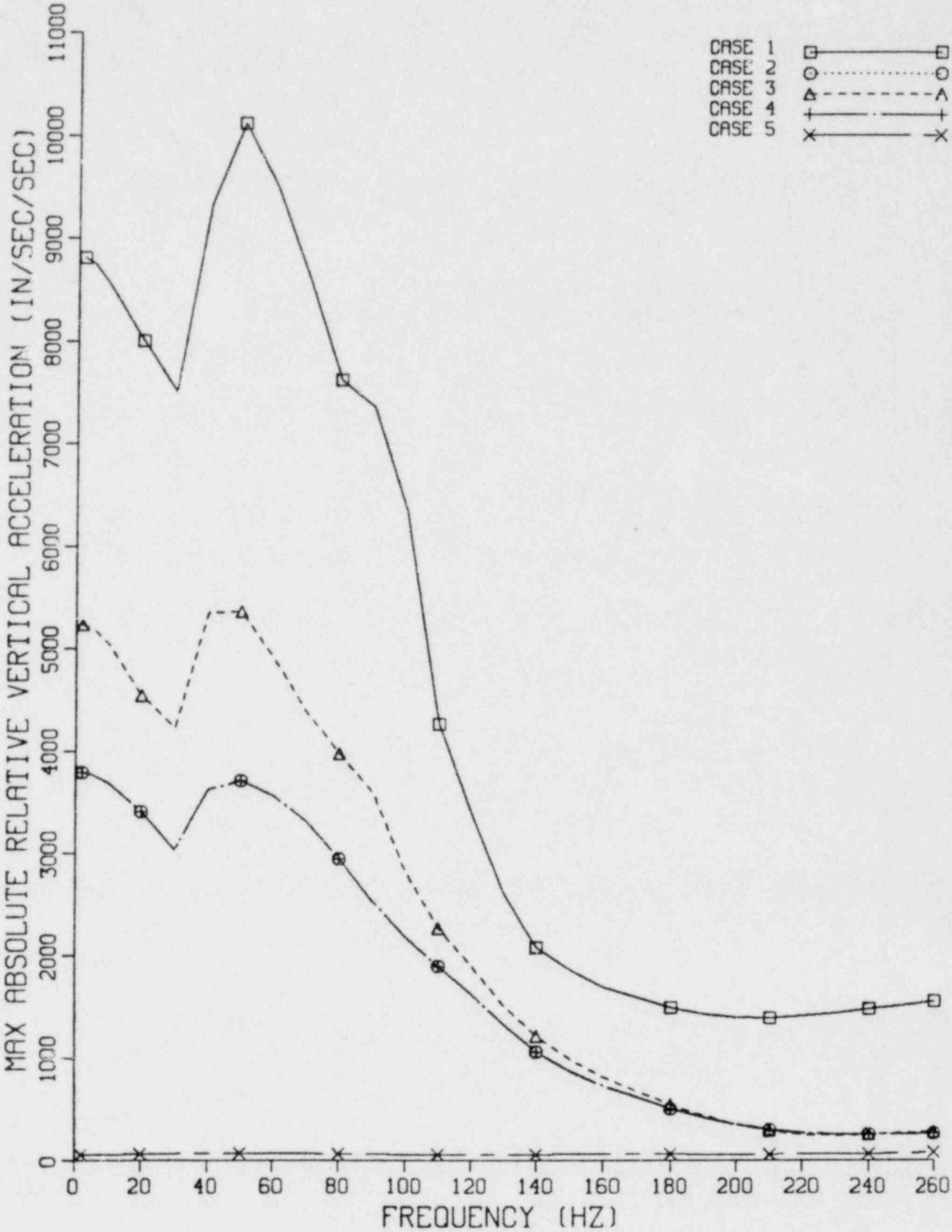

FIGURE 6. Response Spectrum: Maximum Absolute Relative Vertical Acceleration vs Frequency (Preliminary Cases 1 through 5).

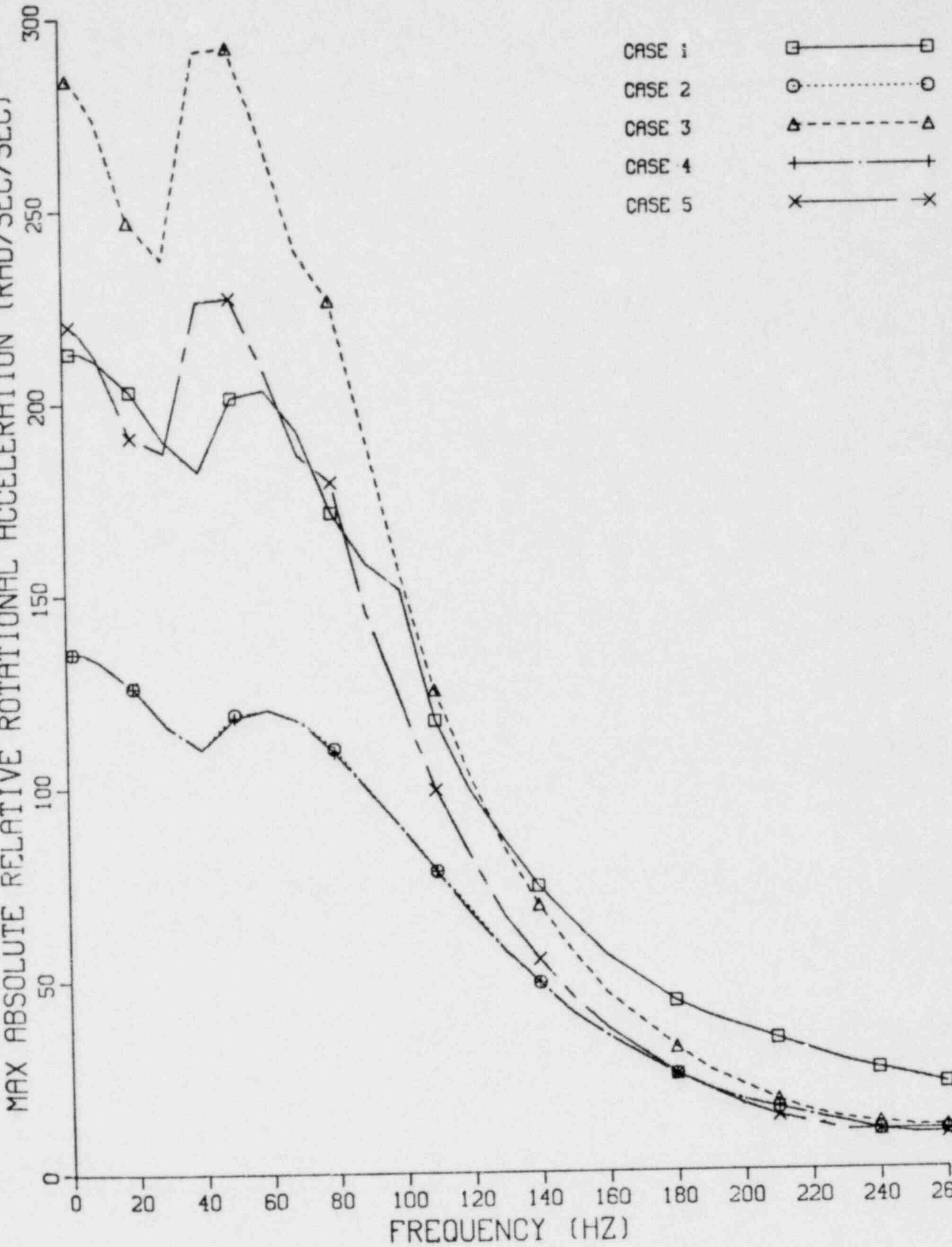

FIGURE 7. Response Spectrum: Maximum Absolute Relative Rotational Acceleration vs Frequency (Preliminary Cases 1 through 5).

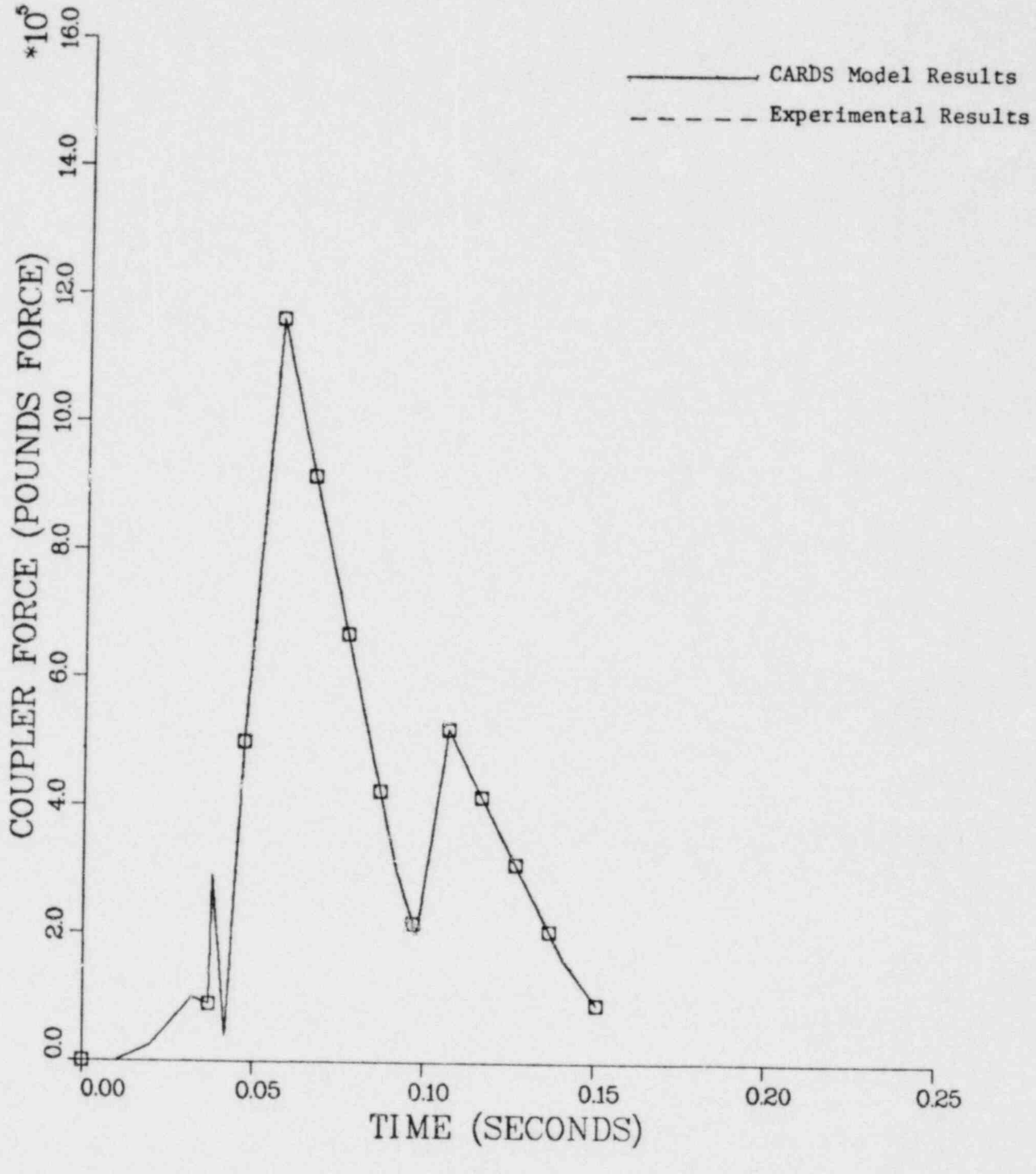

FIGURE 8. Coupler Force vs Time During Impact of Cask-Rail Car with Four Hopper Cars Loaded with Ballast (Test 3 - Instrument 3) (Case 1: Measured Coupler Force).

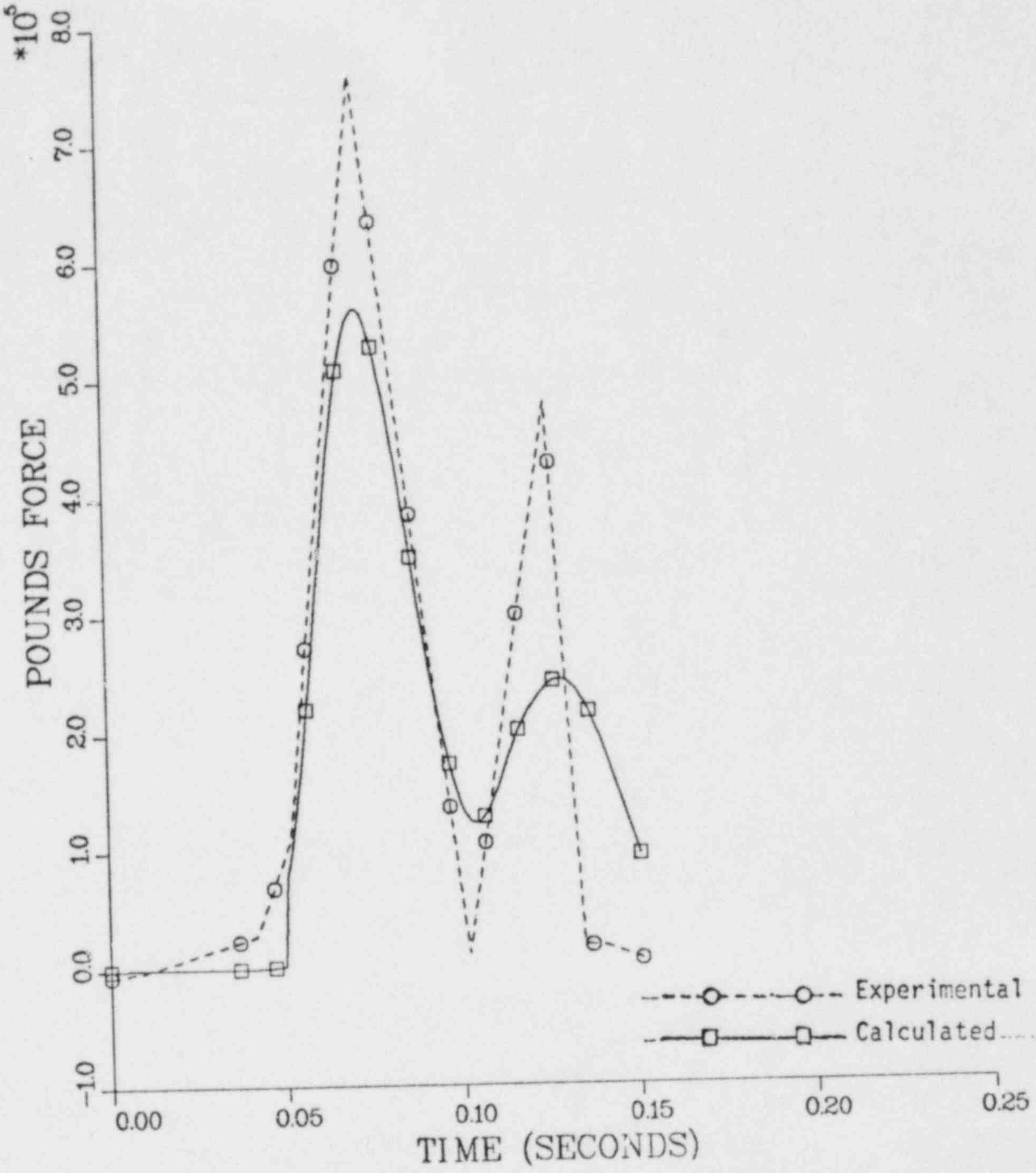

FIGURE 9. Horizontal Force of Interaction Between Cask and Rail Car vs Time During Impact with Four Hopper Cars Loaded with Ballast (Test 3 - Instrument 27) (Case 1: Measured Coupler Force).

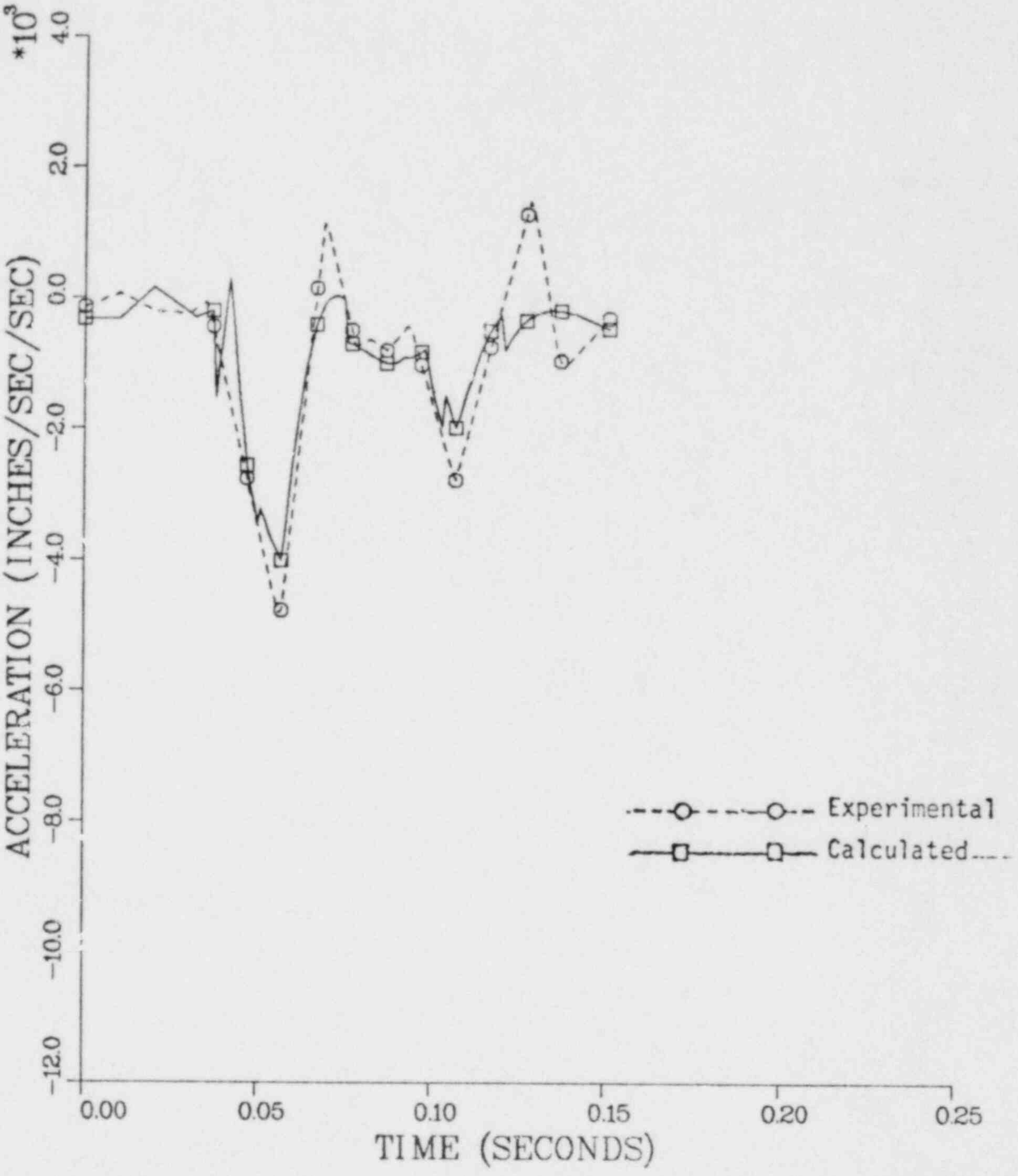

FIGURE 10. Horizontal Acceleration of the Cask-Rail Car During Impact with Four Hopper Cars Loaded with Ballast (Test 3 - Instrument 12: Filtered at 100 Hz) (Case 1: Measured Coupler Force).

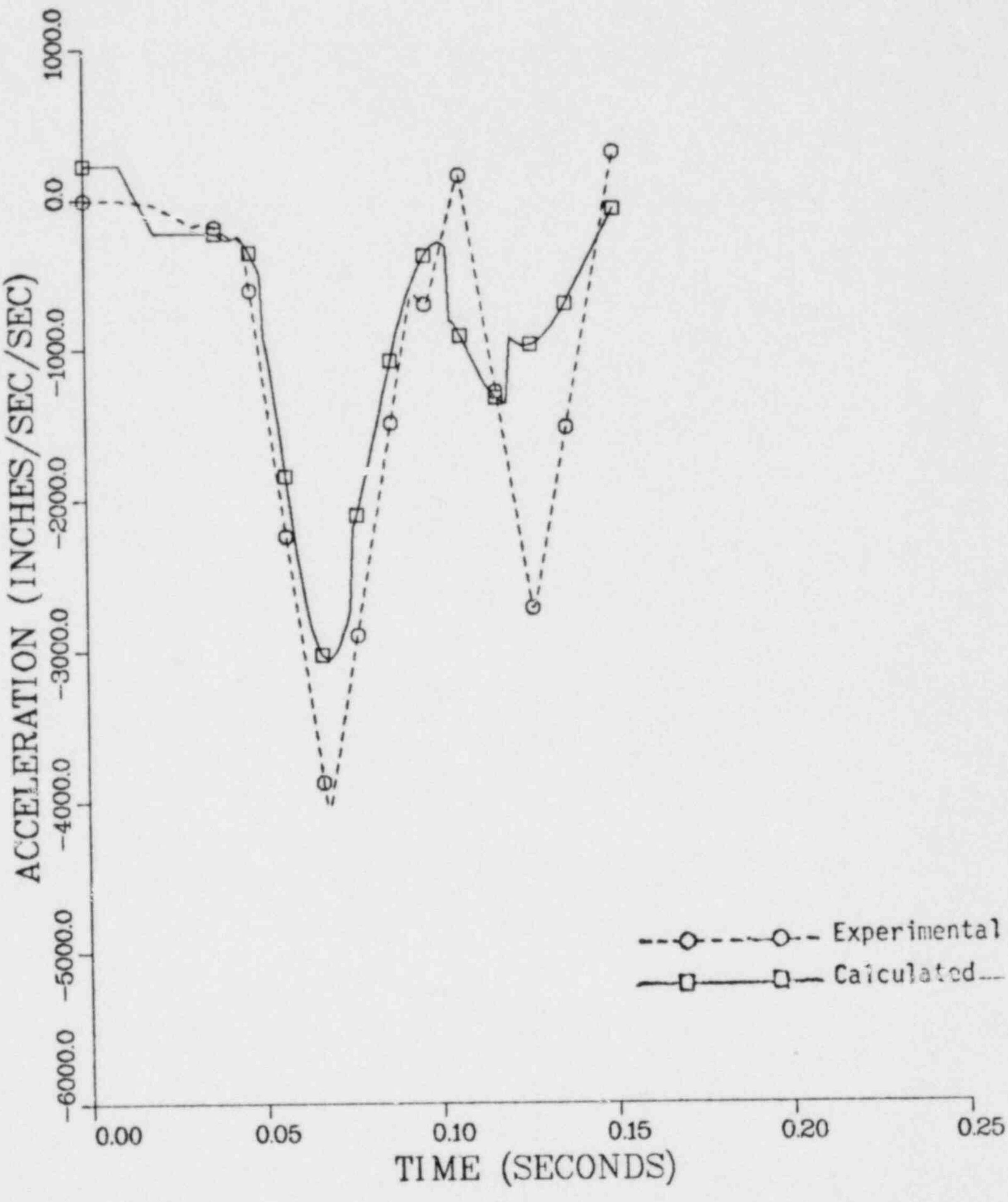

FIGURE 11. Horizontal Acceleration of the Cask During Impact with Four Hopper Cars Loaded with Ballast (Test 3 - Instrument 8: Filtered at 100 Hz) (Case 1: Measured Coupler Force).

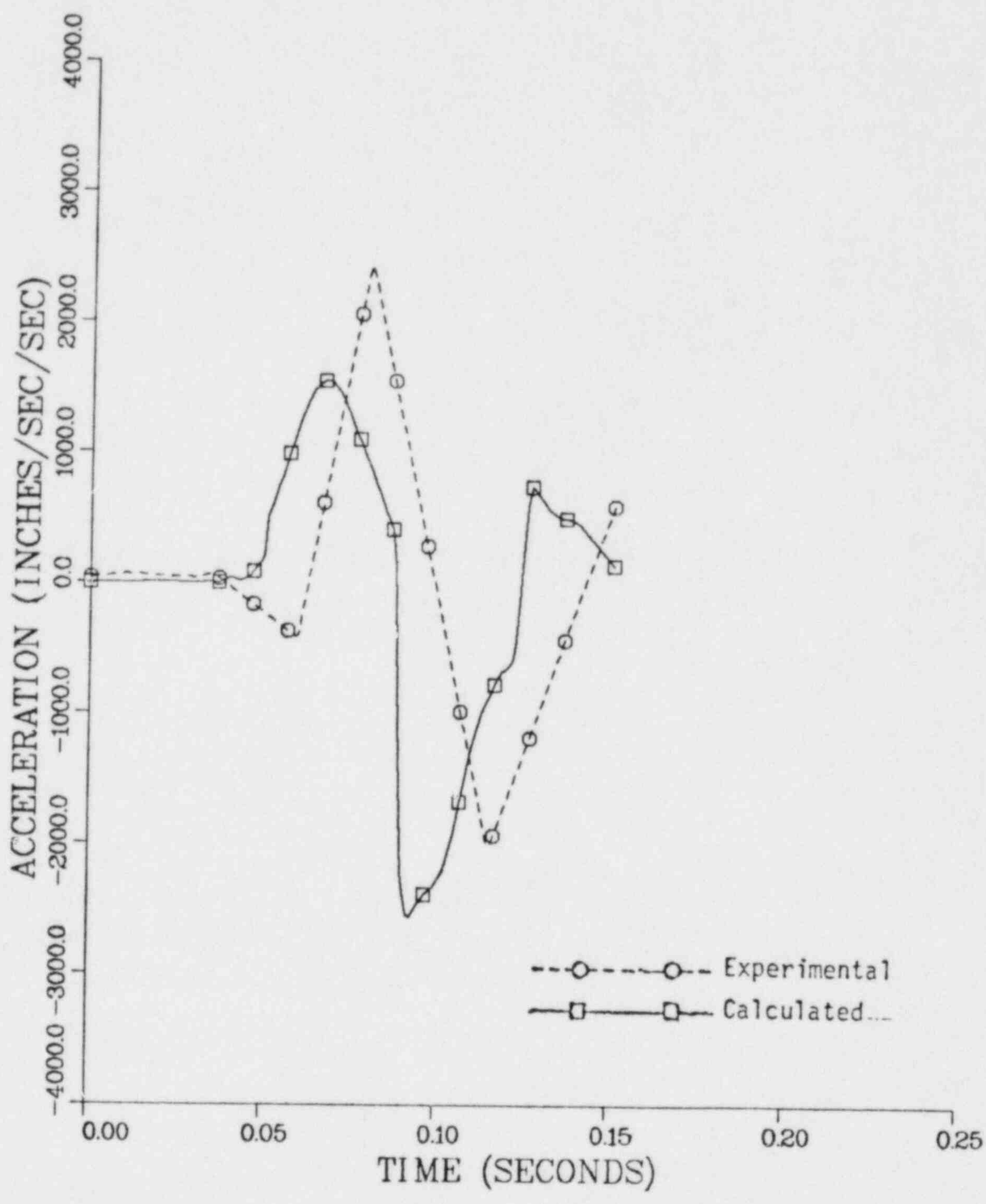

FIGURE 12. Vertical Acceleration of the Cask at the Far End During Impact with Four Hopper Cars Loaded with Ballast (Test 3 - Instrument 11: Filtered at 50 Hz) (Case 1: Measured Coupler Force).

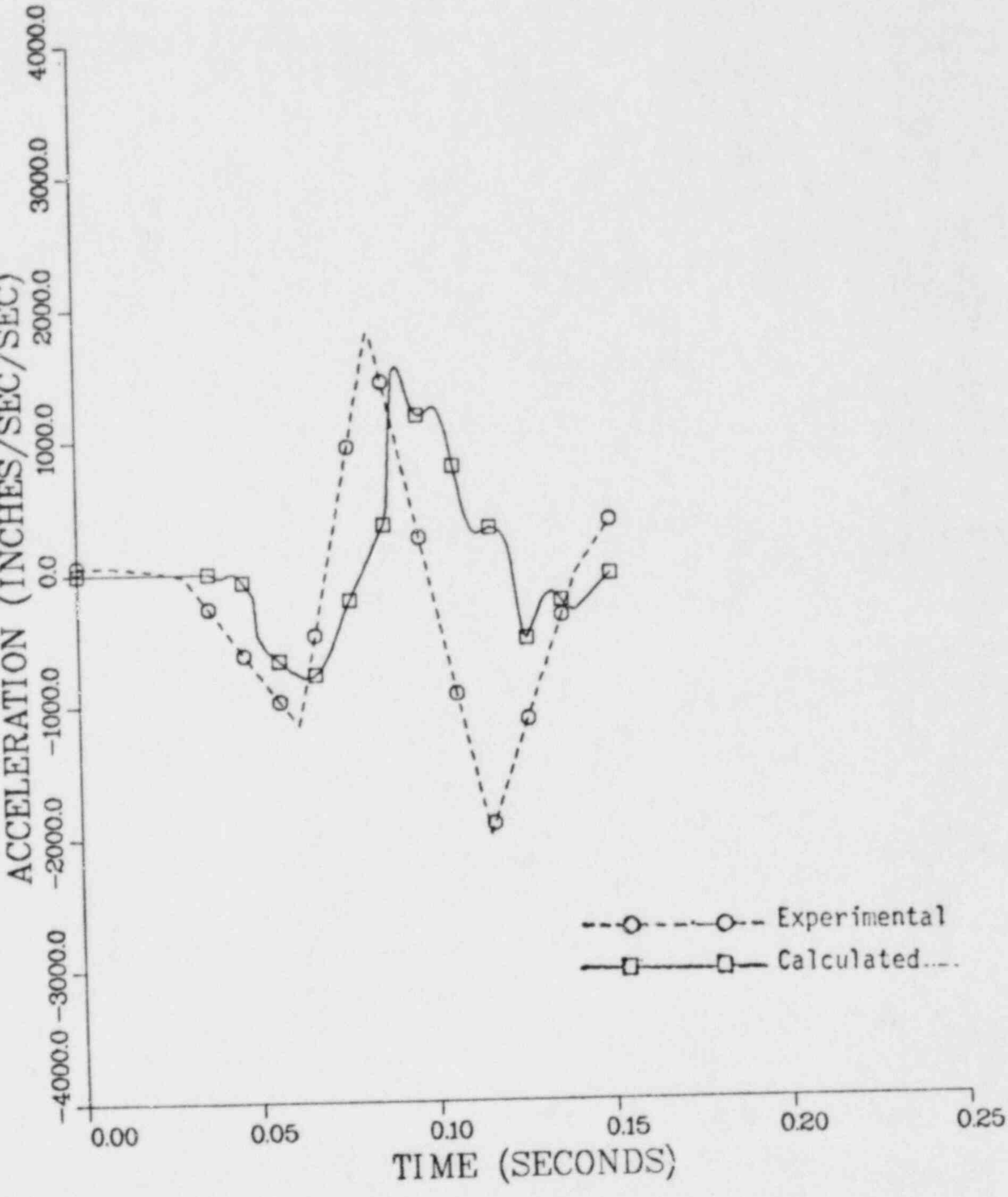

FIGURE 13. Vertical Acceleration of the Cask at the Struck End During Impact with Four Hopper Cars Loaded with Ballast (Test 3 - Instrument 9: Filtered at 50 Hz) (Case 1: Measured Coupler Force).

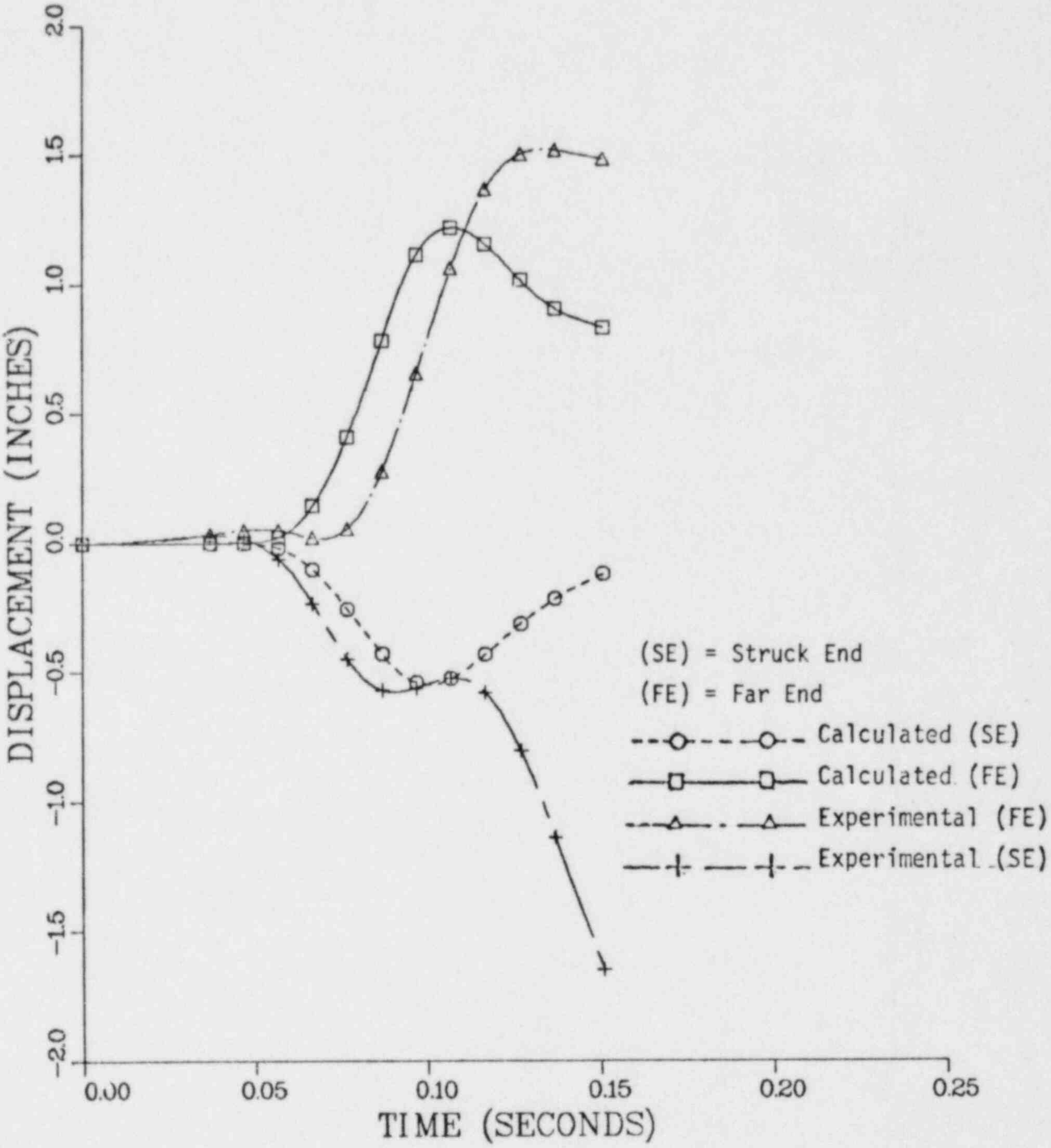

FIGURE 14. Vertical Displacements of the Cask During Impact with Four Hopper Cars Loaded with Ballast (Test 3) (Case 1: Measured Coupler Force).

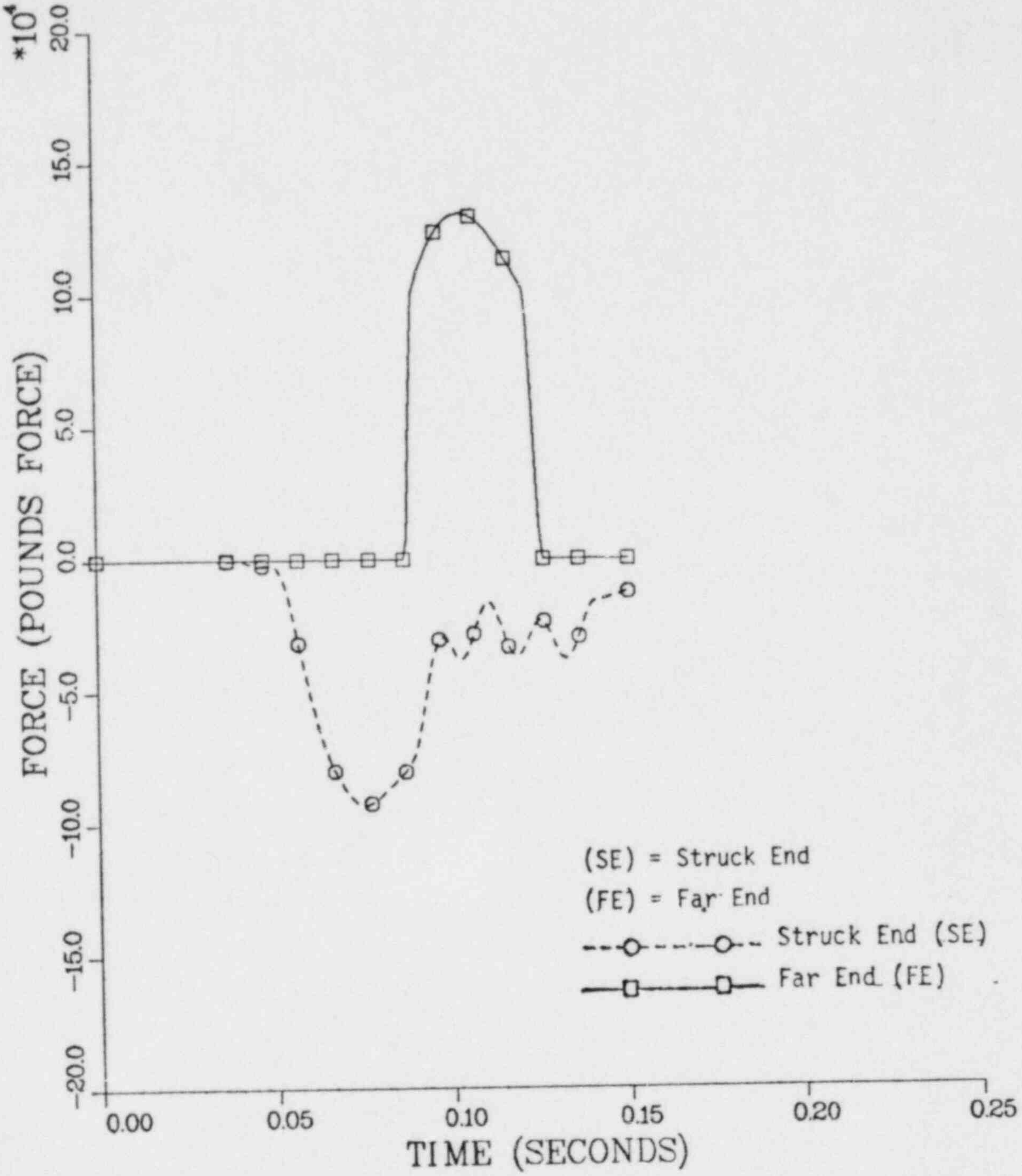

FIGURE 15. Vertical Tiedown Forces During Impact with Four Hopper Cars Loaded with Ballast (Test 3) (Case 1: Measured Coupler Force).

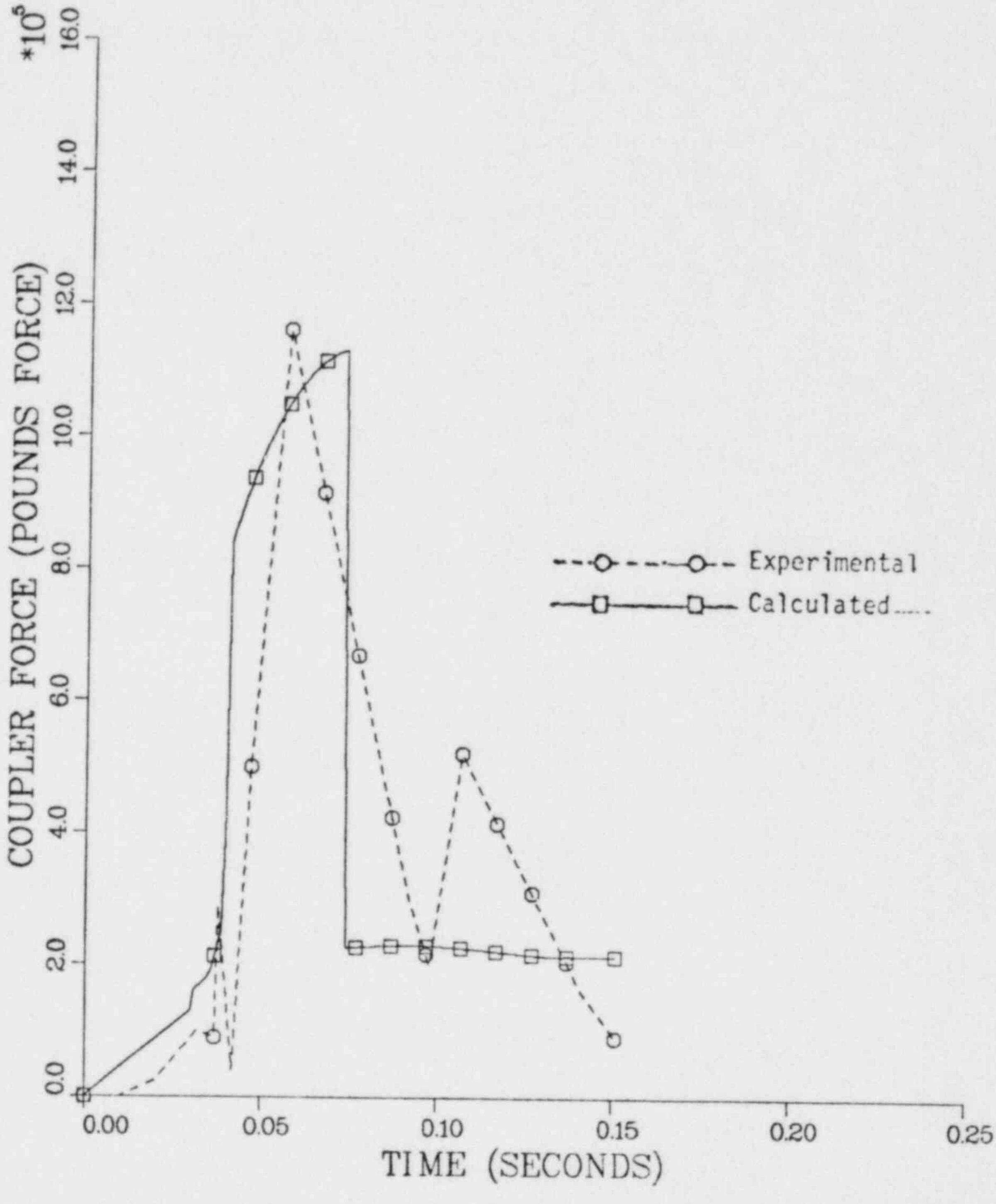

FIGURE 16. Coupler Force vs Time During Impact of Cask-Rail Car with Four Hopper Cars Loaded with Ballast (Test 3 - Instrument 3) (Case 2: Calculated Coupler Force).

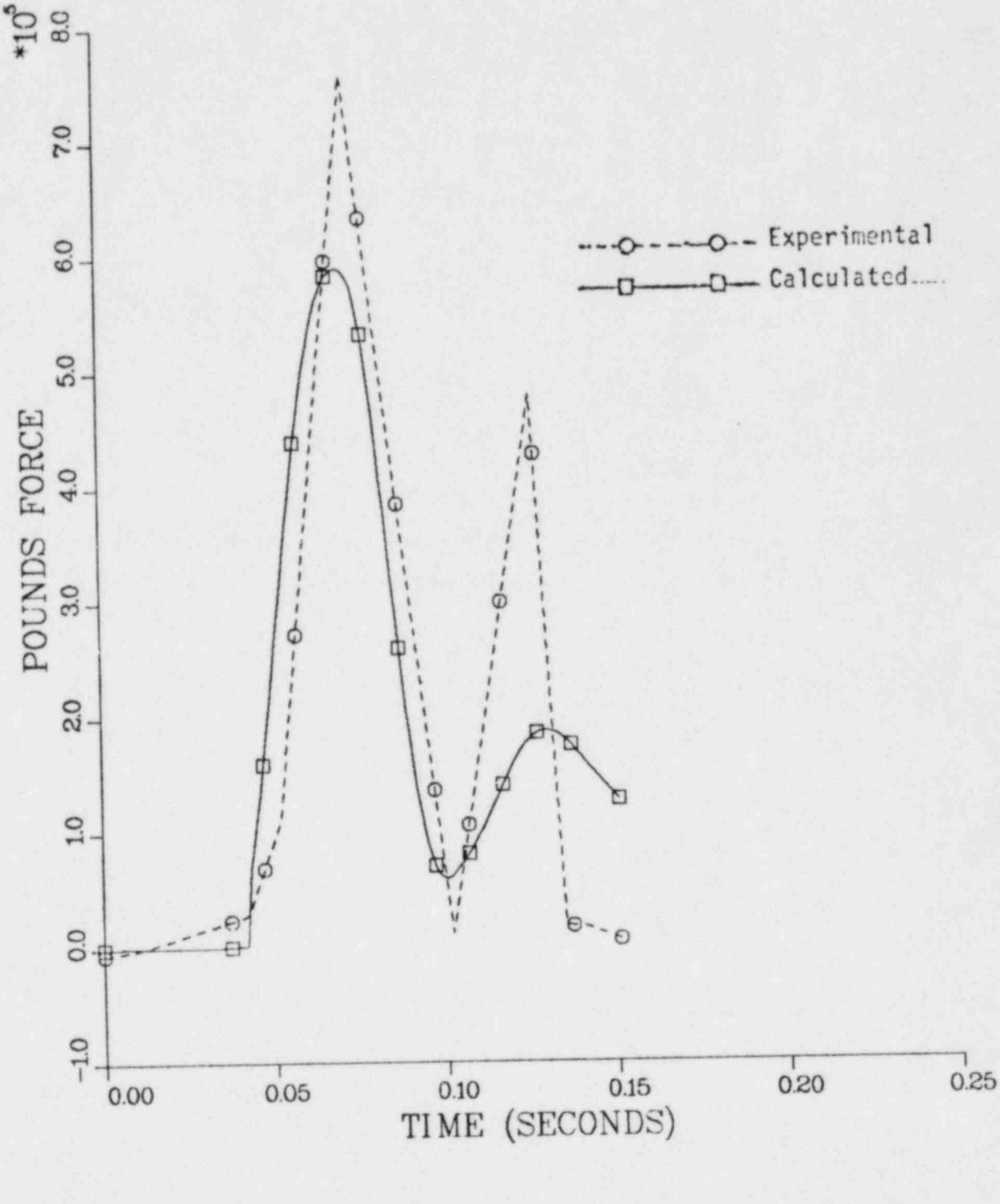

FIGURE 17. Horizontal Force of Interaction Between Cask and Rail Car vs Time During Impact with Four Hopper Cars Loaded with Ballast (Test 3 - Instrument 27) (Case 2: Calculated Coupler Force).

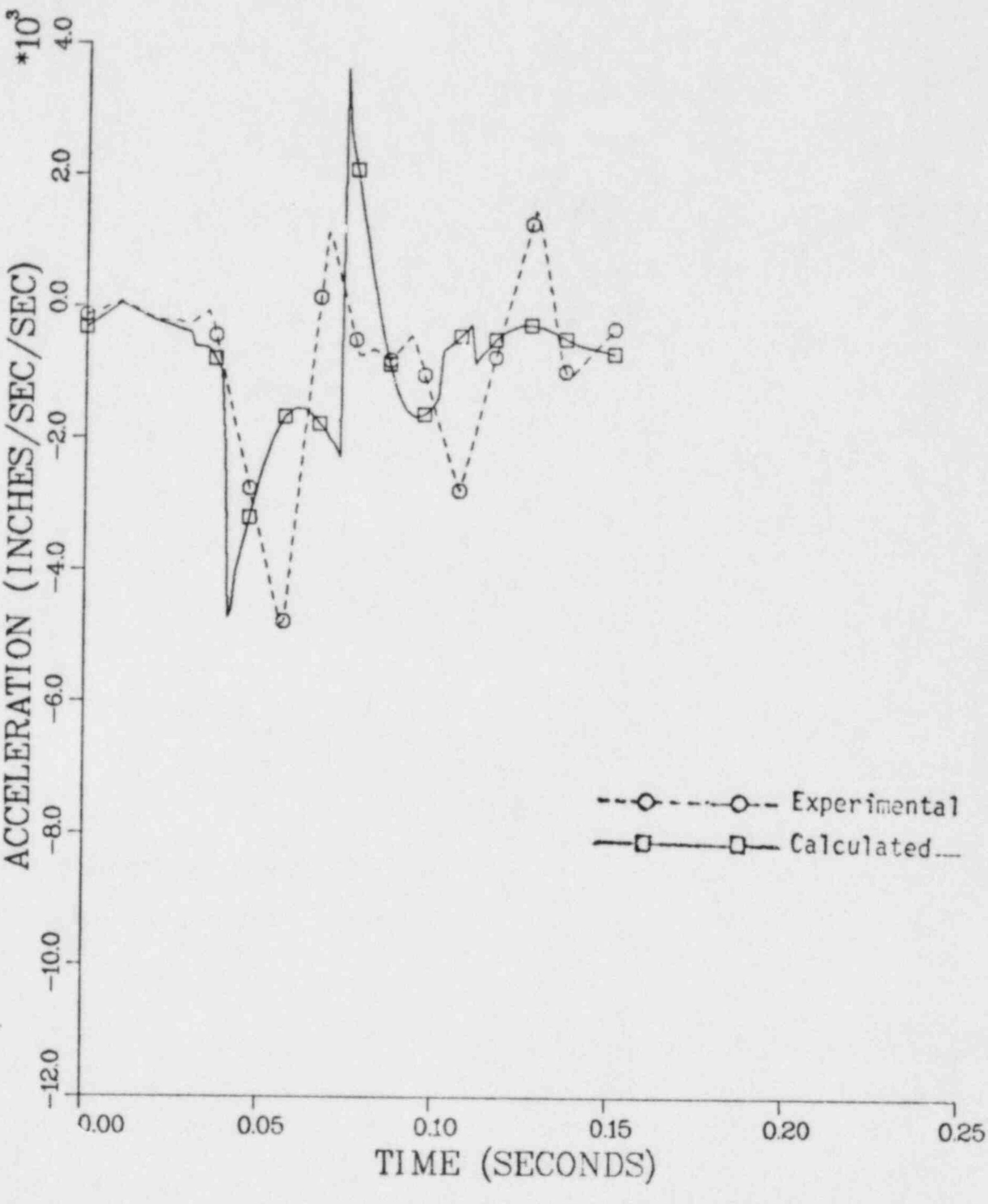

FIGURE 18. Horizontal Acceleration of the Cask-Rail Car During Impact with Four Hopper Cars Loaded with Ballast (Test 3 - Instrument 12: Filtered at 100 Hz) (Case 2: Calculated Coupler Force).

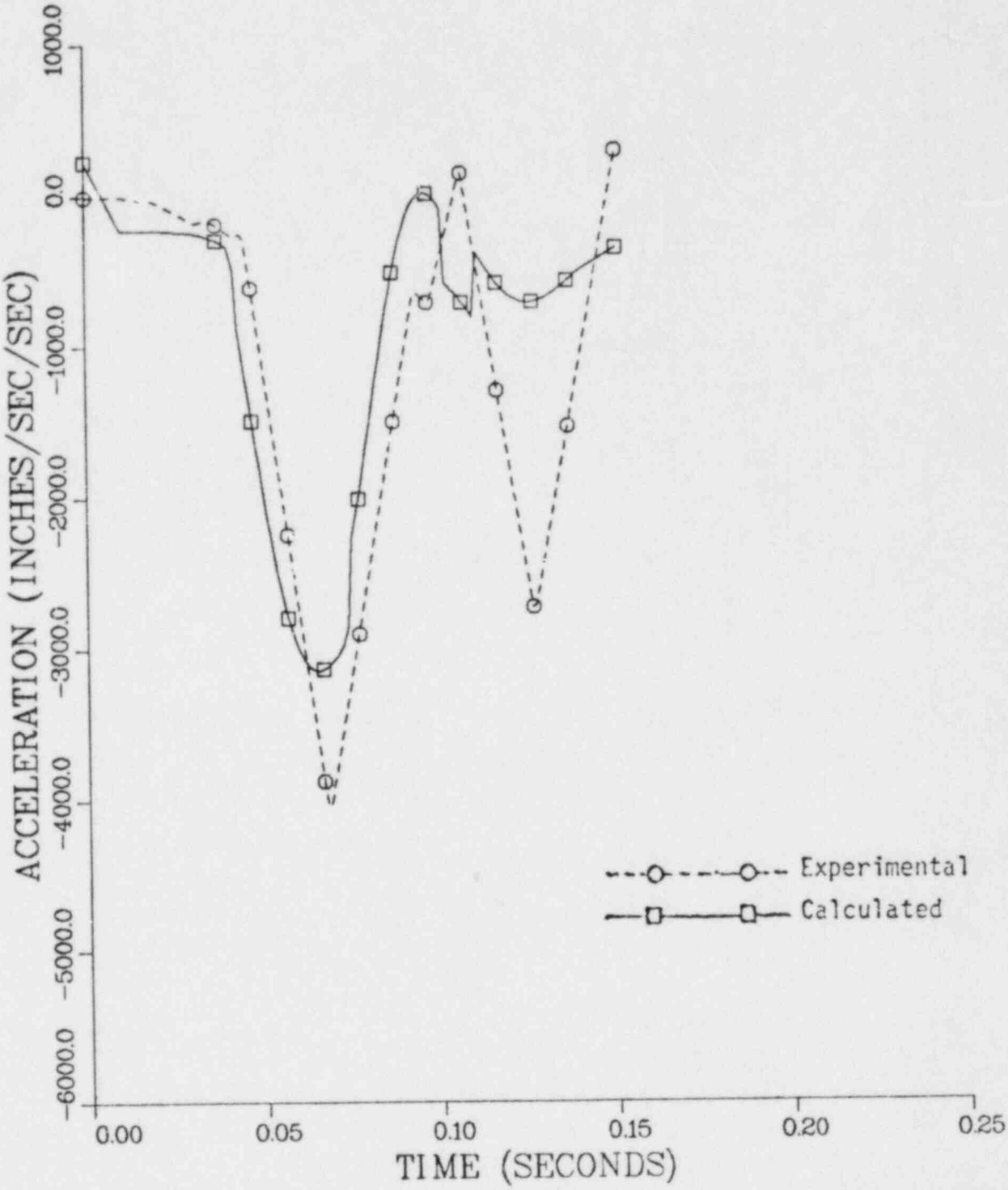

FIGURE 19. Horizontal Acceleration of the Cask During Impact with Four Hopper Cars Loaded with Ballast (Test 3 - Instrument 8: Filtered at 100 Hz) (Case 2: Calculated Coupler Force).

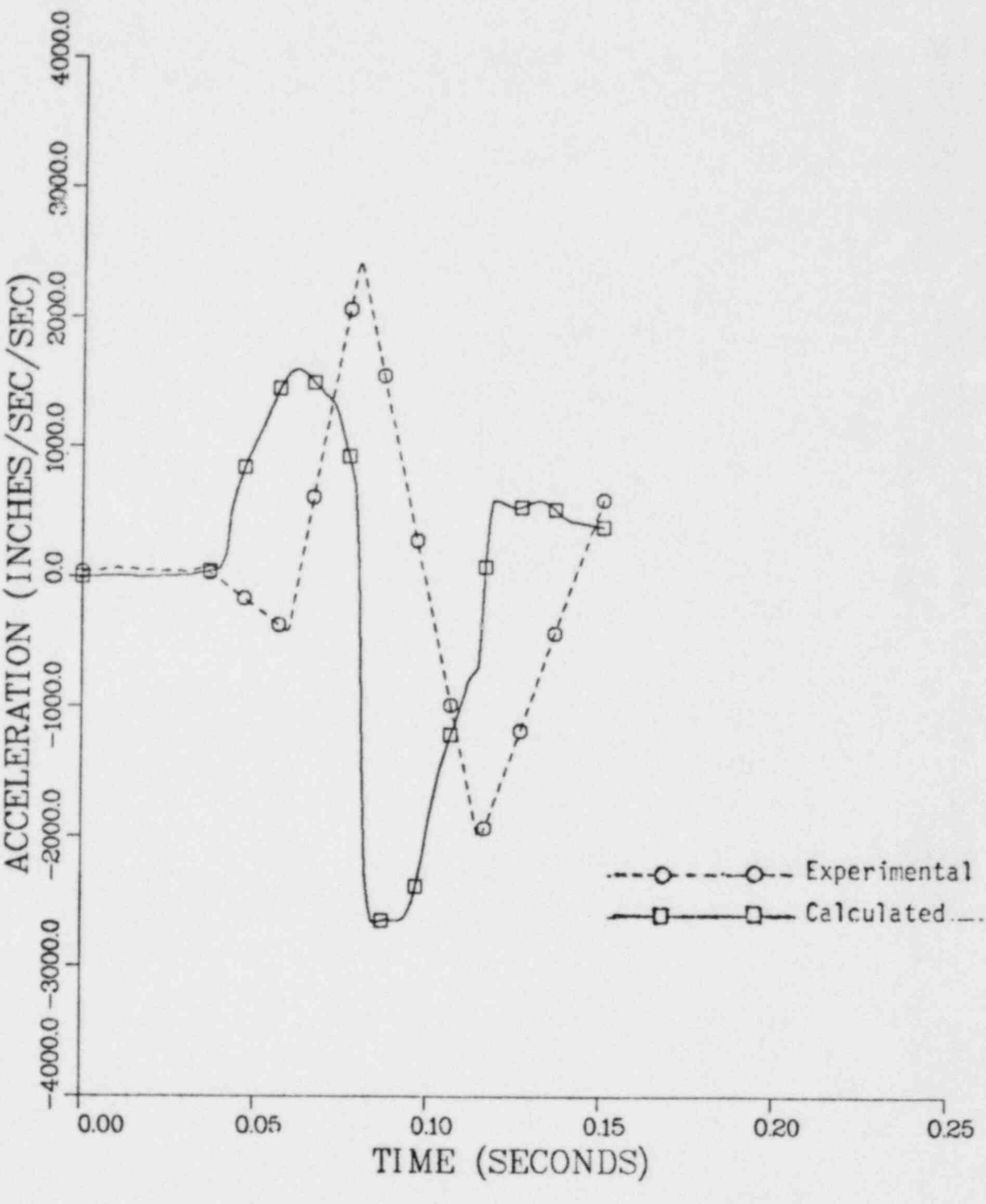

FIGURE 20. Vertical Acceleration of the Cask at the Far End During Impact with Four Hopper Cars Loaded with Ballast (Test 3 - Instrument 11: Filtered at 50 Hz) (Case 2: Calculated Cou; er Force).

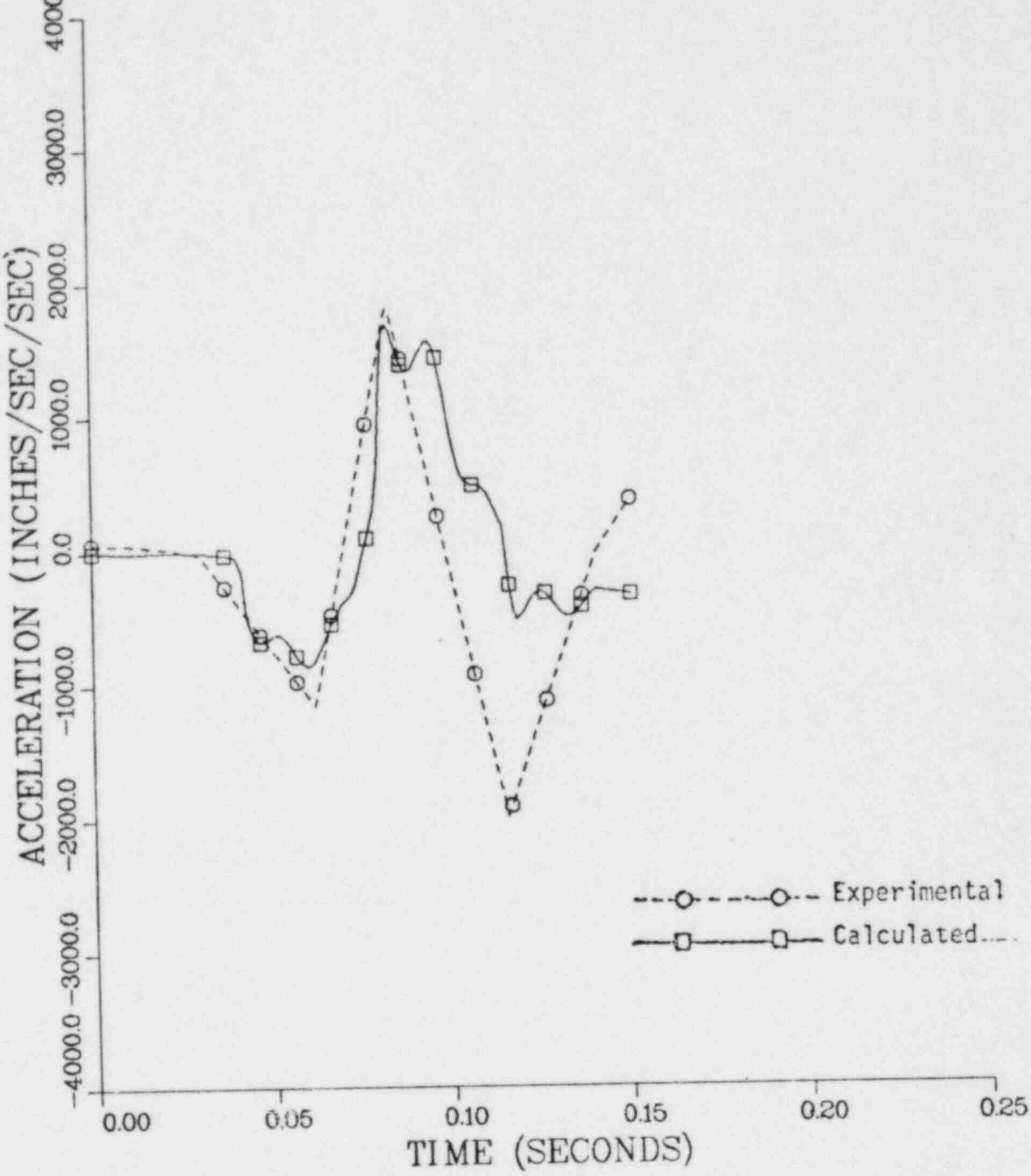

FIGURE 21. Vertical Acceleration of the Cask at the Struck End During Impact with Four Hopper Cars Loaded with Ballast (Test 3 - Instrument 9: Filtered at 50 Hz) (Case 2: Calculated Coupler Force).

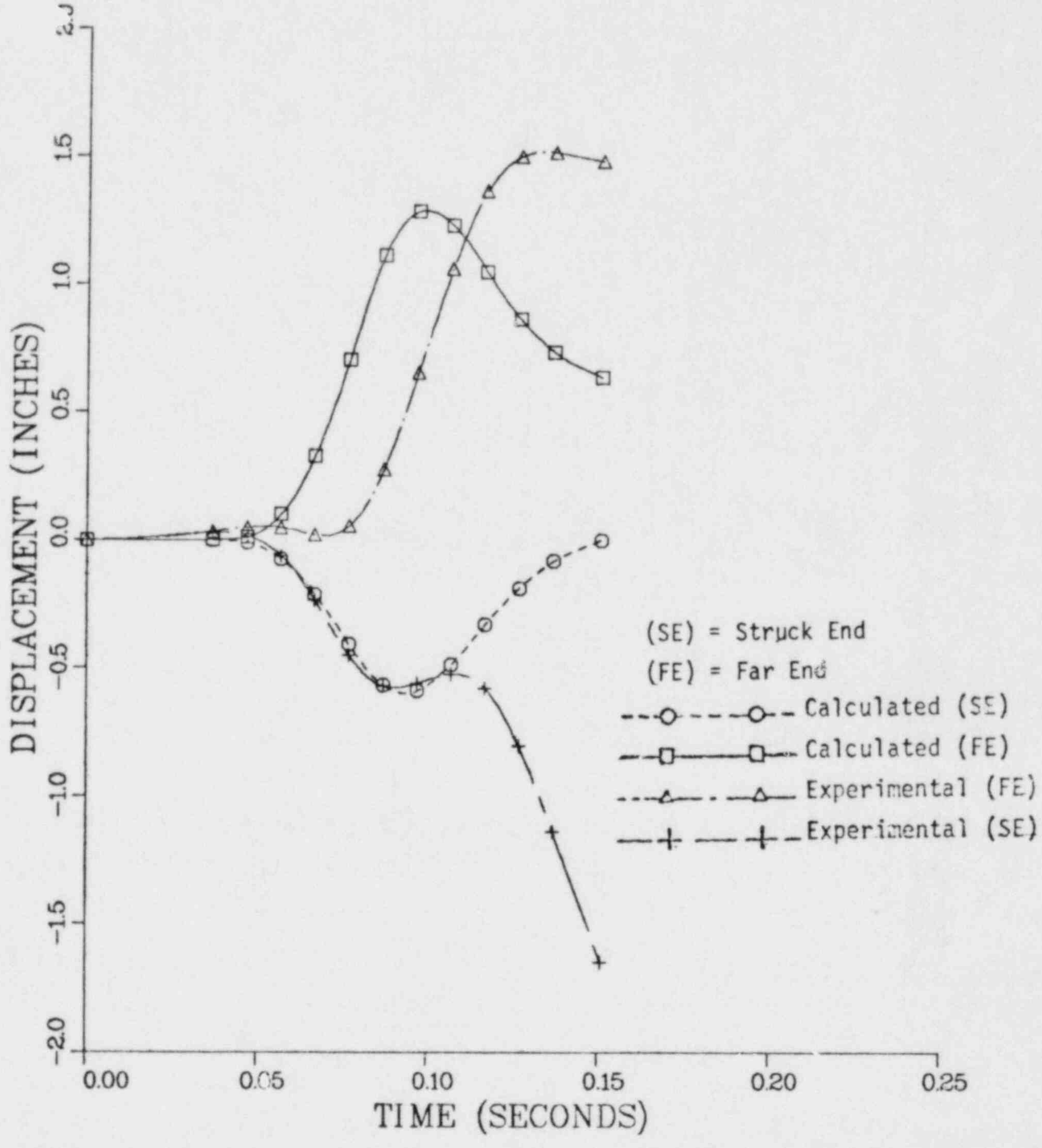

FIGURE 22. Vertical Displacements of the Cask During Impact with Four Hopper Cars Loaded with Ballast (Test 3) (Case 2: Calculated Coupler Force).

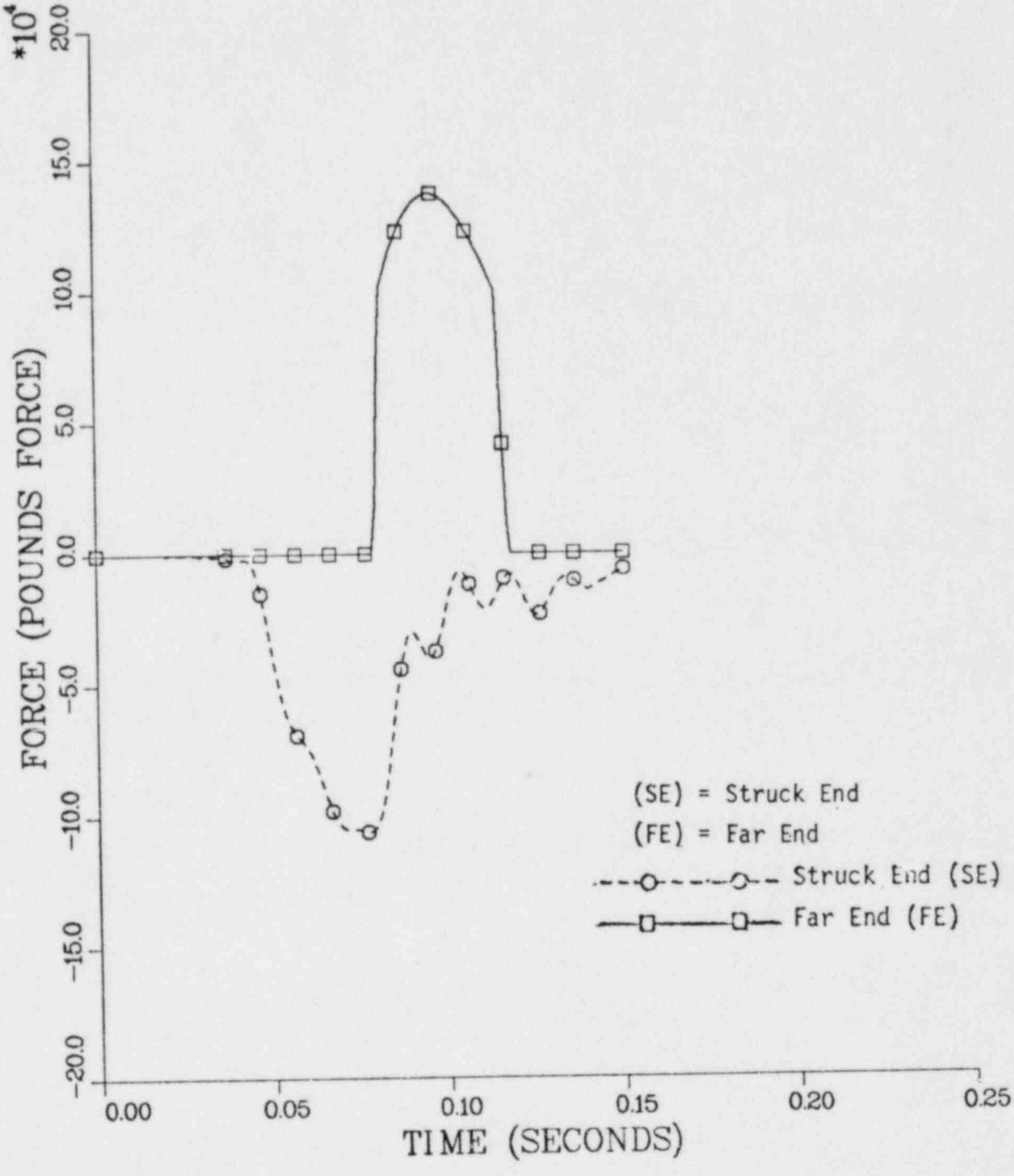

FIGURE 23. Vertical Tiedown Fo~~es During Impact with Four Hopper Cars Loaded with Ballast (Test 3) (Case 2: Calculated Coupler Force).

APPENDIX A

NOMENCLATURE OF TERMS

NOMENCLATURE OF TERMS

C_{S1} through C_{S8} = Damping coefficients for viscous dampers representing structural damping at springs S_1 through S_8 in Figure 1, $\frac{\text{lbs(force)-seconds}}{\text{inch}}$.

DUSCAR = The coupler force calculated by the CARDS model, lbs(force).

DUSX4 = The coupler force obtained from experimental measurements, lbs(force).

DUS1 through DUS8 = The forces acting on springs S_1 through S_8, respectively (see Figure 1), lbs(force).

DWCRF = The frictional force opposing vertical motion of the coupler faces between the hammer car (cask-rail car) and the first car in the anvil train, lbs(force).

DWP1, DWP4 = The frictional forces opposing horizontal motion of the cask on the rail car at the rear and front attachment points, respectively, lbs(force).

DWS1 through DWS8 = Viscous damping forces representing structural damping associated with springs S_1 through S_8, respectively, lbs(force).

k_{SCARS} = A total equivalent spring constant for the combined draft gears of the cask-rail car (hammer car) and the first struck car (anvil car), lbs(force)/inch.

k_{S1} = Stiffness of the horizontal component of the rear tiedown between the cask (M_P) and the rail car (M_{RC}), lbs(force)/inch.

k_{S2} = Stiffness of the vertical component of the rear tiedown between the cask (M_P) and the rail car (M_{RC}), lbs(force)/inch.

k_{S3} = Stiffness of the vertical component of the front tiedown between the cask (M_P) and the rail car (M_{RC}), lbs(force)/inch.

k_{S4} = Stiffness of the horizontal component of the front tiedown between the cask (M_P) and the rail car (M_{RC}), lbs(force)/inch.

k_{S5} = Stiffness of the horizontal component of the cask-rail car suspension at the rear truck, lbs(force)/inch.

k_{S6}, k_{S7} = The spring constants for the equivalent springs representing the rear and front suspensions, respectively, lbs(force)/inch.

k_{S8} = Stiffness of the horizontal component of the cask-rail car suspension at the front truck, lbs(force)/inch.

ℓ_{CF} = Horizontal distance from the vertical centerline of the cask-rail car to the front tiedown attachment point, inches.

ℓ_{CPL} = Horizontal distance from the vertical centerline of the cask-rail car to the coupler face, inches.

ℓ_{CR} = Horizontal distance from the vertical centerline of the cask-rail car to the rear tiedown attachment point, inches.

ℓ_{PF} = Horizontal distance from the vertical centerline of the cask to the front tiedown attachment point, inches.

ℓ_{PR} = Horizontal distance from the vertical centerline of the cask to the rear tiedown attachment point, inches.

ℓ_{RC} = Horizontal distance from the vertical centerline of the cask-rail car to a suspension point at a truck, inches (2*LRC = distance between suspension points.)

M_P = Mass of the cask or package, $\frac{lb_f{}^{*} - sec^2}{inch}$

M_{RC} = Mass of the cask-rail car, $\frac{lb_f - sec^2}{inch}$

sgn(A) = The signum function or sign function.

$$= \begin{cases} +1 & , A > 0 \\ -1 & , A = 0 \\ -1 & , A < 0 \end{cases}$$

W_{P1} = That portion of package weight concentrated at rear (far end) tiedown attachment point, lbs_f.

W_{P4} = That portion of package weight concentrated at front (struck end) tiedown attachment point, lbs_f.

*lbs_f or lb_f = lbs(force)

X_d = The horizontal displacement of an equivalent single-degree-of-freedom (1-DOF) representation of the package-rail car system, the displacement of the package (cask) relative to the rail car, inches.

$\dot{X}_d$ = The relative horizontal velocity of the 1-DOF representation of the package-rail car system, inches/second.

$\ddot{X}_d$ = The relative horizontal acceleration of the 1-DOF representation of the package-rail car system, inches/sec^2.

X_F = The horizontal displacement of the c.g. of the first anvil (struck) car, inches.

X_p = Horizontal displacement of the c.g. of the cask or package, inches.

$\dot{X}_p$ = Horizontal velocity of the c.g. of the cask or package, inches/sec.

$\ddot{X}_p$ = Horizontal acceleration of the c.g. of the cask or package (M_p), inches/sec^2.

X_{RC} = Horizontal displacement of the c.g. of the cask-rail car, inches.

$\dot{X}_{RC}$ = Horizontal velocity of the c.g. of the cask-rail car, inches/sec.

$\ddot{X}_{RC}$ = Horizontal acceleration of the c.g. of the cask-rail car (M_{RC}), inches/sec^2.

X_{RC56} = Horizontal displacement of the cask-rail car at the support point at the rear truck, inches.

$\ddot{X}_{RC56}$ = Horizontal acceleration of the cask-rail car at the support point at the rear truck, inches/sec^2.

X_{RC78} = Horizontal displacement of the cask-rail car at the support point at the front truck, inches.

$\ddot{X}_{RC78}$ = Horizontal acceleration of the cask-rail car at the support point at the front truck, inches/sec^2.

X_{TR}, X_{TF} = Horizontal displacements of the c.g.'s of the rear and front trucks, respectively, on the cask-rail car, inches.

$\ddot{X}_{TR}$, $\ddot{X}_{TF}$ = Horizontal accelerations of the c.g.'s of the rear (M_{TR}) and front (M_{TF}) rail car trucks, respectively, inches/sec^2.

Y_d = The vertical displacement of an equivalent 1-DOF representation of the package-rail car system, the displacement of the package (cask) relative to the rail car, inches.

$\dot{Y}_d$ = The relative vertical velocity of the equivalent 1-DOF model of the package-rail car system, inches/sec.

$\ddot{Y}_d$ = The relative vertical acceleration of the equivalent 1-DOF model of the package-rail car system, inches/sec^2.

Y_{RC} = Vertical displacement of the cask-rail car at its c.g., inches.

$\dot{Y}_{RC}$ = The vertical velocity of the cask-rail car at its c.g., inches/sec.

$\ddot{Y}_{RC}$ = Vertical acceleration of the cask-rail car at its c.g., inches/sec^2.

Y_{RC56}, Y_{RC78} = The vertical displacements of the rail car at the rear and front suspensions, respectively, inches.

$\ddot{Y}_{RC56}, \ddot{Y}_{RC78}$ = The vertical accelerations of the rail car at the rear and front suspensions, respectively, inches/sec^2.

Y_p = Vertical displacement of the c.g. of the cask or package, inches.

$\dot{Y}_p$ = The vertical velocity of the c.g. of the cask or package, inches/sec.

$\ddot{Y}_p$ = Vertical acceleration of the cask or package at its c.g., inches/sec^2.

Z_p = Vertical distance from the horizontal centerline of the cask to its top and bottom surfaces, inches.

Z_{RC} = Vertical distance from the horizontal centerline of the cask-rail car to its top and bottom surfaces, inches.

α_{CPL} = A factor to allow the damping term DWCRF to vary as a function of the absolute value of the coupler force raised to the factor power.

β_{CPL} = A multiplying factor representing the fraction of the coupler force actually applied to the moving coupler faces.

θ_p = The angle of rotation of the X_p and Y_p axes about an axis perpendicular to the X_p - Y_p plane through the c.g. of the cask or package, radians.

$\dot{\theta}_p$ = The angular velocity of the package or cask about an axis through its c.g., radians/sec.

$\ddot{\theta}_p$ = Angular acceleration of the package or cask about an axis through its c.g., radians/sec^2.

θ_{RC} = The angle of rotation of the X_{RC} and Y_{RC} axes about an axis perpendicular to the X_{RC} - Y_{RC} plane through the c.g. of the rail car, radians.

$\dot{\theta}_{RC}$ = The angular velocity of the rail car about an axis through its c.g., radians/sec.

$\ddot{\theta}_{RC}$ = Angular acceleration of the rail car about an axis through its c.g., radians/sec^2.

μ_{CPL} = The coefficient of friction for the sliding of the two coupler faces against each other.

μ_{PR} = The coefficient of friction for the sliding of the package or cask on the rail car.

ω_X = The frequency of vibration for the 1-DOF EOM for the relative horizontal motion of the cask-rail car system, sec^{-1} or Hz.

ω_Y = The frequency of vibration for the 1-DOF EOM for the relative vertical motion of the cask-rail car system, sec^{-1} or Hz.

ΣF_{XP} = The summation of horizontal forces acting on the cask or package, lbs(force).

ΣF_{XRC} = The summation of horizontal forces acting on the rail car, lbs(force).

ΣF_{YP} = The summation of vertical forces acting on the cask, lbs(force).

ΣF_{YRC} = The summation of vertical forces acting on the rail car, lbs(force).

DISTRIBUTION

RT (195)

DOE/RL (6)
P.O. Box 550
Richland, WA 99352

Director, Energy Prog Div (2)
BJ Melton
JD White (3)

DOE/FFTFPO
P.O. Box 550
Richland, WA 99352

Director

DOE/Chicago Patent Office
9800 S. Cass Avenue
Argonne, IL 60439

AA Churm

DOE/Environmental Control and Technology Division
Washington, DC 20545

E.I. Dupont de Nemours and Company
P.O. Box A
Aiken, SC 29801

SF Petry

Los Alamos Scientific Laboratory
P.O. Box 1663
Los Alamos, NM 87545

TD Butler

Pacific Northwest Laboratory
P.O. Box 999
Richland, WA 99352

LD Williams

Sandia Laboratories
P.O. Box 5800
Albuquerque, NM 87115

CF Magnuson

HEDL (37)
P.O. Box 1970
Richland, WA 99352

AG Blasewitz	W/C-31	SJ Mech	W/A-132
DM Bosi	W/A-6	WW Lee	W/C-115
HA Carlson	W/FED-420	RE Lerch	W/C-35
RJ Cash	W/A-6	WE Roake	W/C-16
EA Evans	W/C-23	WF Sheely	W/A-62
SR Fields (14)	W/FED-420	JC Sonnichsen	W/FED-420
JF Fletcher	W/FED-420	HH Yoshikawa	W/C-44
EM Greene	W/FED-420	Central Files (5)	W/C-110
LD Jacobson	W/JAD-7	Publ Services (2)	W/C-115
RL Knecht	W/A-40		

NRC FORM 335 (7-77) U.S. NUCLEAR REGULATORY COMMISSION **BIBLIOGRAPHIC DATA SHEET**		1. REPORT NUMBER (Assigned by DDC) NUREG/CR-1685, Vol. 2 HEDL-TME 80-72	
4. TITLE AND SUBTITLE (Add Volume No., if appropriate) Dynamic Analysis to Establish Normal Shock and Vibration of Radioactive Material Shipping Packages Quarterly Progress Report April 1 1980 - June 30, 1980		2. (Leave blank)	
		3. RECIPIENT'S ACCESSION NO.	
7. AUTHOR(S) S. R. Fields		5. DATE REPORT COMPLETED MONTH September	YEAR 1980
9. PERFORMING ORGANIZATION NAME AND MAILING ADDRESS (Include Zip Code) Hanford Engineering Development Laboratory P.O. Box 1970 Richland, WA 99352		DATE REPORT ISSUED MONTH April	YEAR 1981
		6. (Leave blank)	
		8. (Leave blank)	
12. SPONSORING ORGANIZATION NAME AND MAILING ADDRESS (Include Zip Code) U.S. Nuclear Regulatory Commission Division of Safeguards, Fuel Cycle and Environmental Research Office of Nuclear Regulatory Research Washington, DC 20555		10. PROJECT/TASK/WORK UNIT NO.	
		11. CONTRACT NO. FIN B2263	
13. TYPE OF REPORT Quarterly	PERIOD COVERED (Inclusive dates) April 1, 1980 - June 30, 1980		
15. SUPPLEMENTARY NOTES		14. (Leave blank)	

16. ABSTRACT (200 words or less)

An equation of motion was derived for an equivalent single-degree-of-freedom representation of the relative rotational motion between a radioactive material shipping package (cask) and its rail car (support). This equation of motion, along with those derived earlier for the relative horizontal and vertical motion, was used to construct CARRS (Cask-Rail Car Response Spectra Generator), a model to generate frequency response spectra using calculated results obtained from the CARDS (Cask Rail Car Dynamic Simulator) model. Frequency response spectra are presented for various exploratory cases. Further evaluation of the performance of CARDS was made, after insertion of the latest parameter data, by comparing calculated results with response variables measured during Test 3 of the series of tests conducted at the Savannah River Laboratories.

17. KEY WORDS AND DOCUMENT ANALYSIS	17a. DESCRIPTORS

17b. IDENTIFIERS/OPEN-ENDED TERMS

18. AVAILABILITY STATEMENT	19. SECURITY CLASS (This report)	21. NO. OF PAGES
Unlimited	Unclassified	
	20. SECURITY CLASS (This page) Unclassified	22. PRICE $